Geoscience Frontiers 10 (2019) 2063–2084

HOSTED BY

Contents lists available at ScienceDirect

China University of Geosciences (Beijing)

Geoscience Frontiers

journal homepage: www.elsevier.com/locate/gsf

Research Paper

Late syn- to post-collisional magmatism in Madagascar: The genesis of the Ambalavao and Maevarano Suites

Donnelly B. Archibald [a,b,*], Alan S. Collins [b], John D. Foden [b], Justin L. Payne [c], Peter Holden [d], Théodore Razakamanana [e]

[a] Department of Earth Sciences, St. Francis Xavier University, Physical Sciences Complex, 5009 Chapel Square, Antigonish, NS, B2G 2W5, Canada
[b] Centre for Tectonics, Resources and Exploration (TRaX), Department of Earth Sciences, The University of Adelaide, Adelaide 5005, SA, Australia
[c] Centre for Tectonics, Resources and Exploration (TRaX), School of Built and Natural Environments, University of South Australia, Mawson Lakes, SA, 5001, Australia
[d] Research School of Earth Sciences, The Australian National University, Canberra, ACT, 2601, Australia
[e] Département des Sciences de la Terre, Université de Toliara, Toliara, 601, Madagascar

ARTICLE INFO

Article history:
Received 5 October 2017
Received in revised form
16 April 2018
Accepted 22 July 2018
Available online 19 September 2018

Keywords:
Madagascar geology
East African orogen
Zircon geochronology
Zircon oxygen and hafnium isotopes
Post-collisional magmatism

ABSTRACT

The East African Orogen involves a collage of Proterozoic microcontinents and arc terranes that became wedged between older cratonic blocks during the assembly of Gondwana. The Ediacaran–Cambrian Ambalavao and Maevarano Suites in Madagascar were emplaced during the waning orogenic stages and consist of weakly deformed to undeformed plutonic rocks and dykes of mainly porphyritic granite but also gabbro, diorite and charnockite. U-Pb geochronological data date emplacement of the Ambalavao Suite to between ca. 580 Ma and 540 Ma and the Maevarano Suite to between ca. 537 Ma and 522 Ma. Major and trace element concentrations are consistent with emplacement in a syn- to post-collisional tectonic setting as A-type (anorogenic) suites. Oxygen ($\delta^{18}O$ of 5.27‰–7.45‰) and hafnium ($\varepsilon_{Hf}(t)$ of −27.8 to −12.3) isotopic data from plutons in the Itremo and Antananarivo Domains are consistent with incorporation of an ancient crustal source. More primitive $\delta^{18}O$ (5.27‰–5.32‰) and $\varepsilon_{Hf}(t)$ (+0.0 to +0.2) isotopic values recorded in samples collected from the Ikalamavony Domain demonstrate the isotopic variation of basement sources present in the Malagasy crust. The Hf isotopic composition of Malagasy zircon are unlike more juvenile Ediacaran–Cambrian zircon sources elsewhere in the East African Orogen and, as such, Madagascar represents a distinct and identifiable detrital zircon source region in Phanerozoic sedimentary provenance studies. Taken together, these data indicate that high-T crustal anatexis, crustal assimilation and interaction of crustal material with mantle-derived melts were the processes operating during magma emplacement. This magmatism was coeval with polyphase deformation throughout Madagascar during the amalgamation of Gondwana and magmatism is interpreted to reflect lithospheric delamination of an extensive orogenic plateau.

1. Introduction

Late syn- to post-collisional plutons are common in the East African Orogen (EAO) (Jacobs et al., 2008; Bingen et al., 2009; Goodenough et al., 2010). The EAO formed during the Ediacaran–Cambrian amalgamation of the supercontinent Gondwana, and is one of the planet's largest orogens (Stern, 1994; Stern, 2002; Meert, 2003; Collins and Pisarevsky, 2005; Johnson et al., 2011; Fritz et al., 2013; Blades et al., 2015; Merdith et al., 2017; da Silva Schmitt et al., 2018). The northern part of the EAO (the Arabian-Nubian Shield; ANS) consists of a pre-Neoproterozoic continental terrane (the Afif Terrane), surrounded by many Neoproterozoic oceanic-arc terranes (Johnson et al., 2011; Robinson et al., 2014) that sutured together in the Ediacaran (Cox et al., 2012). In the Mozambique Belt to the south (Fritz et al., 2013), the EAO is the collision zone between the Indian Dharwar Craton and the African Congo-Tanzania-Bangweulu Block (Fig. 1a). In the ANS, many oceanic suture zones tie together the various terranes (Robinson et al., 2014, 2015; Blades et al., 2015, 2017) but the

* Corresponding author. Department of Earth Sciences, St. Francis Xavier University, Physical Sciences Complex 2060, 5009 Chapel Square, Antigonish NS, B2G 2W5, Canada.
E-mail address: darchiba@stfx.ca (D.B. Archibald).
Peer-review under responsibility of China University of Geosciences (Beijing).

https://doi.org/10.1016/j.gsf.2018.07.007

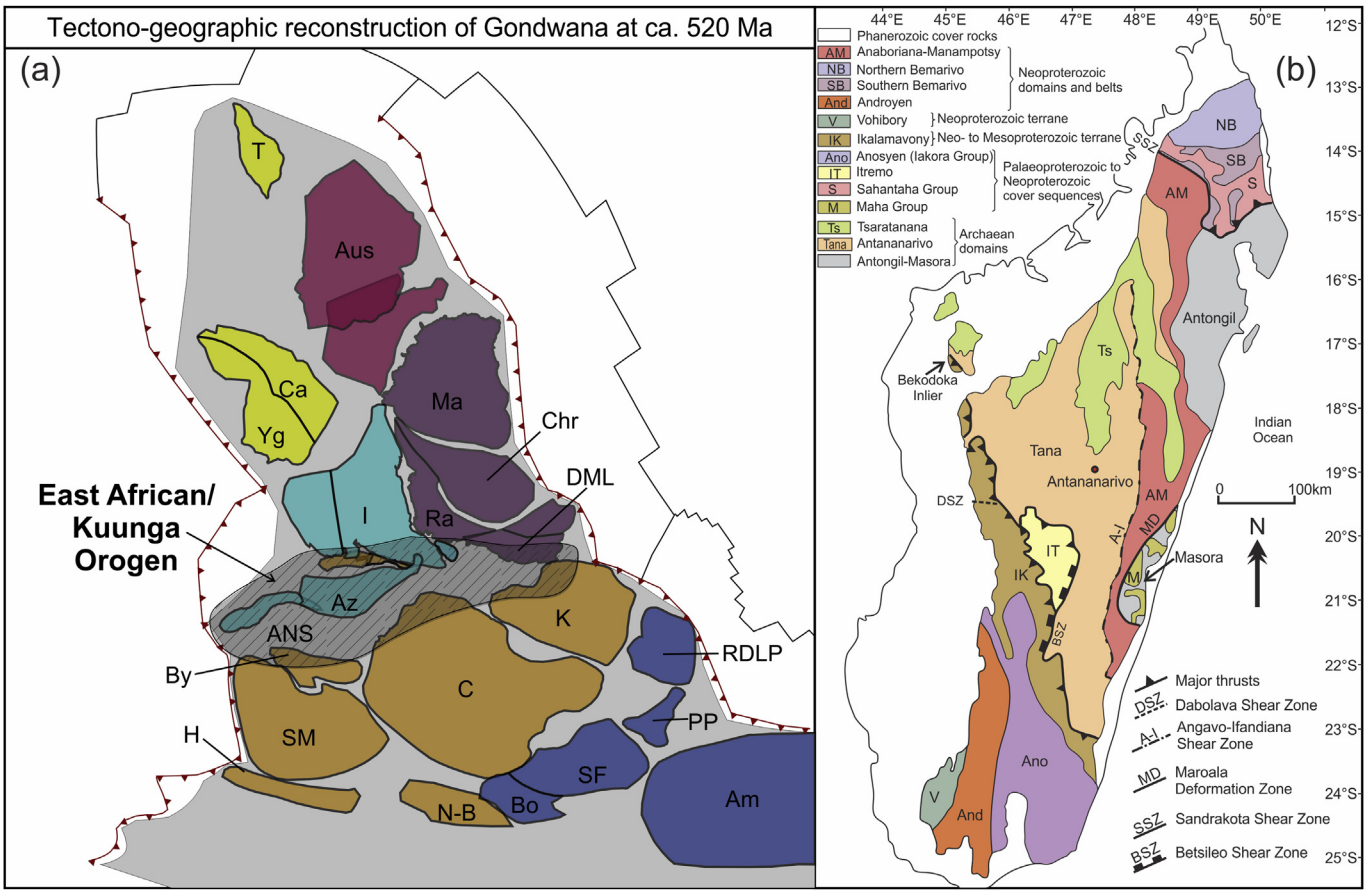

Figure 1. (a) Tectono-geographic reconstruction at ca. 520 Ma showing the location of the East African-Kuunga Orogen (modified from Merdith et al., 2017). Shaded grey area is inferred extent of Gondwana shelf and is meant as a guide only. The longitude is arbitrary and unconstrained. The cratonic crust is coloured (online version) by present day geography: South America, dark blue; India and the Middle East, light blue; China, yellow; Africa, orange; Australia, crimson; Antarctica, purple. (b) Simplified basement geology of Madagascar (after Collins, 2006 and De Waele et al., 2011). The location of the Dabolava Shear Zone is from CGS (2009). Abbreviations: Am, Amazonia; Az, Azania; Bo, Borborema; By, Bayuda; Ca, Cathaysia (South China); C, Congo-Tanzania-Bangweulu Block; Chr, Chron Craton; DML, Dronning Maud Land (Antarctica); H, Hoggar; I India (Dharwar Craton); K, Kalahari; Ma, Mawson; N-B, Nigeria-Benin; PP, Paranapanema; Ra, Rayner (Antarctica); RDLP, Rio de la Plata; SF, São Francisco; SM, Sahara Metacraton.

location of potential suture zones becomes more complicated to the south (Shackleton, 1996). Unlike Phanerozoic orogens that typically involve accretion of multiple terranes (e.g. the Appalachians of eastern North America; van Staal et al., 2009), Shackleton (1996) posited that the Mozambique Ocean closed to form a single suture in East Africa. Collins and Windley (2002) considered a single-suture model to be an over-simplification, and that a band of pelitic gneisses with late-Neoproterozoic depositional ages in Madagascar represented another Mozambique Ocean suture zone (the Betsimisaraka Suture) and it separated central Madagascar from India. Tucker et al. (2011) questioned the presence of such a suture and instead proposed that Madagascar was part of a 'Greater Dharwar Craton' that incorporated all of eastern and central Madagascar on the margin of India, thus, reverting to a single suture hypothesis for the Mozambique Ocean (Tucker et al., 2011).

Elucidating the tectonic setting of central Madagascar during the Ediacaran to Cambrian is therefore, critical to understanding the tectonic geography of the formation of central Gondwana. Here, we focus on the geochemistry of voluminous Ediacaran and Cambrian plutonic rocks of the Ambalavao and Maevarano Suites in Madagascar, in part, to compare with analogous data from elsewhere in the EAO that were used to constrain the late-orogenic tectonic setting (e.g. Jacobs et al., 2008; Bingen et al., 2009). New zircon U-Pb and both O and Hf isotopic data coupled with whole-rock geochemical data provide new insights into the petrogenesis of the Ambalavao and Maevarano Suites between 18°S and 22°S in central Madagascar. These data are also important for detrital zircon studies in a broad range of Phanerozoic clastic sediment sequences possibly sourced from the EAO (e.g. Squire et al., 2006; Martin et al., 2017) in that Madagascar may represent a unique source region for isotopically evolved Ediacaran–Cambrian detrital zircon.

2. Precambrian geology of Madagascar

Madagascar contains several Precambrian to earliest Palaeozoic 'basement' units overlain by Phanerozoic sedimentary and volcanic rocks (Collins, 2006; Roig et al., 2012). The oldest rocks are located along Madagascar's east coast in the Palaeoarchaean to Palaeoproterozoic Antongil and Masora Domains (Fig. 1b) that are considered remnants of the Dharwar Craton of southern India (Tucker et al., 1999; Schofield et al., 2010; Armistead et al., 2018). The Antananarivo Domain underlies most of central Madagascar. Within it, ca. 2550–2500 Ma granitoids (the Betsiboka Suite) are tectonically interlayered with paragneiss that were thermally reworked between ca. 850 Ma and 500 Ma coincident with the development of shallowly dipping gneissic fabrics that pre-date intrusion of Ediacaran–Cambrian plutons (Moine et al., 2014). Later, discrete shear zones developed syn- to post-magmatism (Collins et al., 2003c). Overlying these older rocks are Proterozoic metasedimentary rocks of the Itremo Group (Cox et al., 2004), the Ambatolampy Group in the Antananarivo Domain (Archibald et al.,

2015), the Maha Group in the Masora Domain (De Waele et al., 2011), the Iakora Group in southern Madagascar (Boger et al., 2014), and the Andrarona (Bauer et al., 2011) and Sahantaha Groups (De Waele et al., 2011) in northern Madagascar.

The Ikalamavony Domain is a N–NW trending unit in west Madagascar (Figs. 1b and 2) that consists of Stenian–early Tonian orthogneiss and paragneiss rocks (GAF-BGR, 2008d; CGS, 2009) that were intruded by the ca. 1080–980 Ma Dabolava Suite (CGS, 2009; Archibald et al., 2018). These rocks may correlate with the newly discovered "TOAST" Terrane in east Dronning-Maud Land, Antarctica (Jacobs et al., 2015). Geochronological data and field evidence in the Ikalamavony Domain indicates that sedimentation, volcanism and magmatism occurred simultaneously (CGS, 2009; Archibald et al., 2018).

The Antananarivo, Itremo and Ikalamavony Domains amalgamated prior to ca. 850 Ma before they were intruded by the

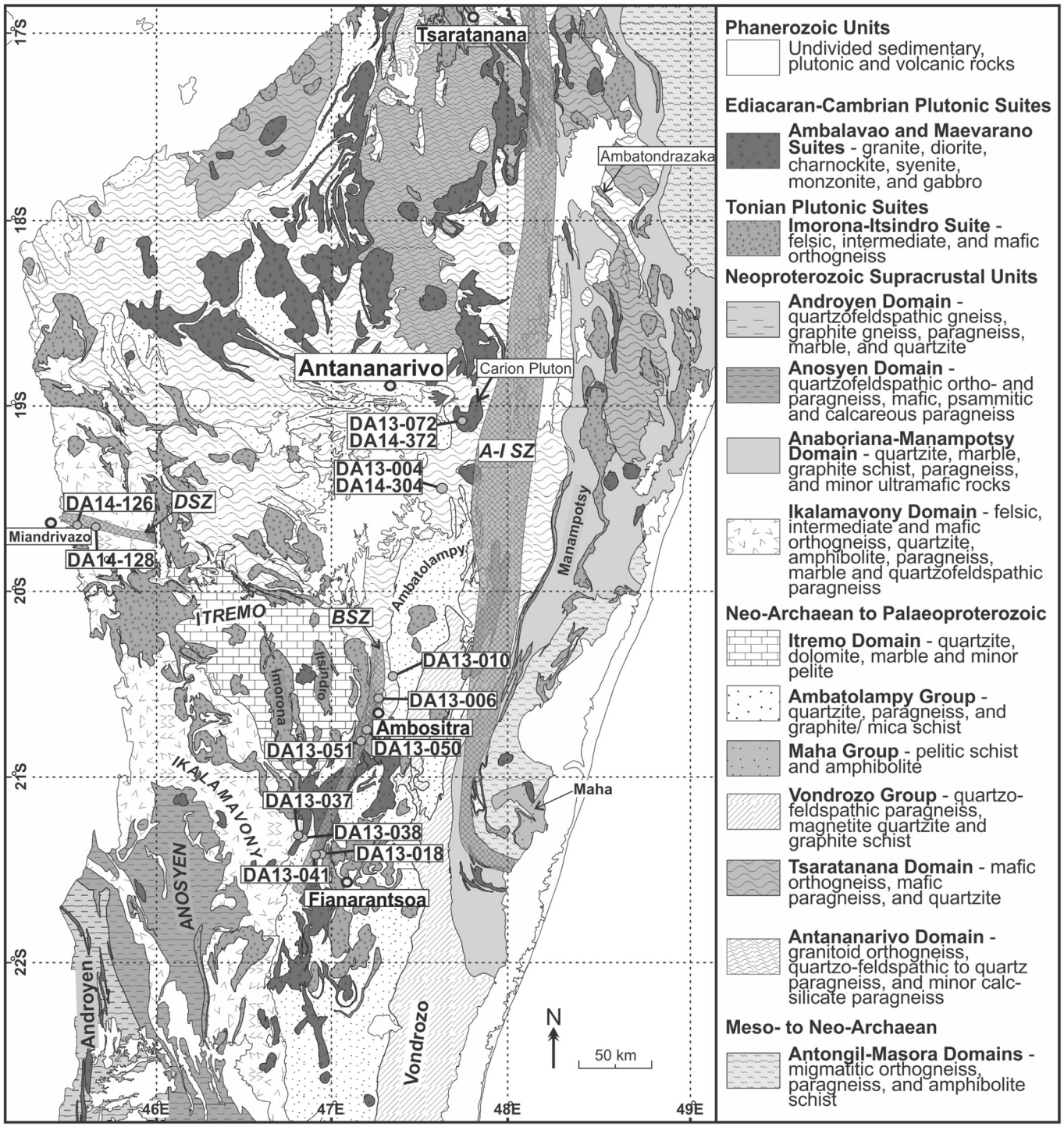

Figure 2. Geologic map of central Madagascar (modified after Roig et al., 2012) showing the extent of Ediacaran to Cambrian magmatism sampled in this study. The Sofia Group crops out in the northern Antananarivo Domain but is not distinguished from the other units in the domain. Location of the Betsileo Shear Zone (BSZ) is from Collins (2006), the Dabolava Shear Zone (DSZ) from CGS (2009) and the Angavo-Ifandiana Shear Zone (A-I SZ) from Raharimahefa et al. (2013).

Table 1
Summary of sample names, lithology, locations and geographical reference for samples of the Ambalavao and Maevarano Suites.

Sample	Domain	Latitude (°S)	Longitude (°E)	Lithology	Textures	Mineralogy
Maevarano Suite						
DA13-004	Antananarivo	19°22′08.7″	47°27′25.8″	Granite	fg massive	af + qtz + pl + bt + cpx + am + op + zrc + all
DA13-006	Antananarivo	20°30′28.0″	47°14′55.2″	Granodiorite	mg-cg massive	af + qtz + pl + bt + cpx + am + op + zrc + all + tit
Ambalavao Suite						
DA13-010	Antananarivo	20°18′13.8″	47°18′47.3″	Granite	mg-cg massive	af + qtz + pl + bt + cpx + am + op + zrc + all
DA13-018	Antananarivo	21°15′40.4″	46°49′31.3″	Monzogranite	fg-mg massive	af + qtz + pl + bt + cpx + am + op + zrc + all
DA13-037	Antananarivo	21°15′18.1″	46°43′03.1″	Granite	weakly foliated	af + qtz + pl + bt + op + zrc
DA13-038	Antananarivo	21°15′14.7″	46°43′58.3″	Granite	weakly foliated	af + qtz + pl + bt + op + zrc + all
DA13-041	Antananarivo	21°15′49.7″	46°45′56.7″	Granite	fg-mg massive	af + qtz + pl + bt + cpx + am + op + zrc + all
DA13-050	Itremo	20°39′13.8″	47°09′54.8″	Granite	mg-cg weakly foliated	af + qtz + pl + bt + op + zrc + all
DA13-051	Itremo	20°40′04.1″	47°09′01.6″	Granite	mg-cg porphyritic	af + qtz + pl + bt + op + zrc + all + tit
DA13-072	Antananarivo	18°54′05.9″	47°41′28.6″	Syenogranite	porphyritic	af + qtz + pl + bt + am + op + zrc
DA14-126	Ikalamavony	19°32′53.2″	45°28′09.0″	Granite	mg-cg porphyritic foliated	af + qtz + pl + bt + op + zrc + all
DA14-128	Ikalamavony	19°34′10.3″	45°29′28.7″	Granite	mg-cg porphyritic	af + qtz + pl + bt + op + zrc + all

Abbreviations: fg = fine-grained, mg = medium-grained, cg = coarse-grained, af = alkali-feldspar, pl = plagioclase, qtz = quartz, am = amphibole, bt = biotite, cpx = clinopyroxene, zrc = zircon, op = opaque minerals, all = allanite, tit = titanite.

Imorona-Itsindro Suite (Archibald et al., 2016, 2017). The ca. 850–750 Ma plutonic rocks consist mostly of granitoid and gabbro that intruded all central Madagascar domains except the Antongil Domain (see Archibald et al., 2017 for a recent summary). The plutonic suite has isotopic and geochemical characteristics compatible with emplacement in a continental arc (Boger et al., 2014; Archibald et al., 2016, 2017).

The Bemarivo Domain is an exotic terrane in north Madagascar consisting of Proterozoic metasedimentary rocks (Sahantaha Group) and juvenile Tonian–Cryogenian calc-alkaline igneous rocks of the ca. 760 Ma Antsirabe Nord and the ca. 720 Ma Manambato Suites (Thomas et al., 2009). These magmatic arcs coalesced and, along with the Sahantaha Group, were thrust southward over the Antananarivo-Antongil Domain between ca. 540 Ma and 520 Ma (Thomas et al., 2009).

The Neoproterozoic Anaboriana-Manampotsy Domain (Fig. 1b) forms the boundary between the Antongil, Masora and Antananarivo Domains (Roig et al., 2012). This domain was previously interpreted as the Betsimisaraka Domain or suture zone (Collins, 2006). The southern Manampotsy Belt consists of orthogneiss and paragneiss rocks that were deposited on the continental shelf of the Antananarivo Domain (Key et al., 2011). An alternative interpretation is that the Manampotsy Group was deposited into a long, narrow, intracontinental basin during mid-Neoproterozoic time (Tucker et al., 2011). The depositional age of the Manampotsy Group is between ca. 840 Ma and ca. 780 Ma based on the youngest detrital zircon age, syn-depositional volcanic rocks (Tucker et al., 2011), and the age of the intrusive rocks of the Imorona-Itsindro Suite (BGS-USGS-GLW, 2008; Archibald et al., 2016). Granitoid rocks comprise most of the northern Anaboriana Belt (approximately 70% of the surface area) and the remaining 30% is high-grade paragneiss and migmatite of the Bealanana Group (BGS-USGS-GLW, 2008).

3. The Ambalavao and Maevarano Suites

Published classifications for the two magmatic suites are based primarily on the geographical distribution and age (BGS-USGS-GLW, 2008; Goodenough et al., 2010; Zhou et al., 2015). It is challenging, without geochronological data, to distinguish between these magmatic suites based on field relationships, because both plutonic suites contain similar lithologies and are undeformed compared to older plutonic rocks belonging to the Imorona-Itsindro, Dabolava or Betsiboka suites. The term Ambalavao Suite does not represent a single, co-genetic magma but was a term used to signify an Ediacaran magmatic episode across Madagascar between ca. 580 Ma and 540 Ma (BGS-USGS-GLW, 2008; CGS, 2009). The Maevarano Suite (ca. 537–522 Ma) rocks are often distinguished in the field from older intrusive rocks because of the weak foliation development in these rocks since their emplacement occurred late syn- or post-deformation (Goodenough et al., 2010).

Except for the apparent restricted geographical distribution of the Maevarano Suite to the northern Antananarivo, Anaboriana and Bemarivo Domains and the timing of intrusion, discernible differences within these magmatic suites are equivocal, especially since rocks with magmatic crystallisation ages younger than ca. 540 Ma are found throughout Madagascar, but were classified as part of the Ambalavao Suite (refer to Fig. 15 in Tucker et al., 2014). Clearly more work is required to determine whether emplacement of these magmatic suites persisted in the same tectonic environment or whether they represent two distinct magmatic pulses in different tectonic environments. This contribution focuses on the overall petrogenesis of the Ediacaran–Cambrian magmatism in central Madagascar and the elucidation the subtle differences and naming of these suites is beyond the scope of the paper. For our purpose, we follow previous work in that Ambalavao Suite samples are plutonic rocks with crystallisation ages between ca. 580 Ma and 540 Ma and Maevarano Suite samples have younger ages between ca. 537 Ma and 520 Ma, regardless of their geochemical composition or geographical distribution. Undated rock samples plotted on geochemical diagrams are discriminated based on their classification in previous studies.

All but four samples (DA13-004, DA13-072, DA14-126 and DA14-128) under study were collected near the Betsileo Shear Zone (Fig. 2). This shear zone is a post-630 Ma extensional detachment between the Itremo and Antananarivo Domains with a top-to-the-west sense of shear (Collins et al., 2000, 2003b). Samples DA13-004 and DA13-072 were collected to the west the Angavo-Ifandiana Shear Zone (Fig. 2). Samples DA14-126 and DA14-128 were collected near the Dabolava Shear Zone (CGS, 2009) in the Ikalamavony Domain. This shear zone is interpreted as a thrust and the plutons experienced ductile deformation at their margins during late-syn to post-emplacement (CGS, 2009). Ediacaran plutons were hot and therefore, behaved in a ductile manner during thrusting of the pluton over the Ikalamavony Group metasedimentary rocks.

Pluton margins commonly display a foliation that is broadly parallel to the regional fabrics but the foliation typically weakens until plutons become unfoliated in their interiors. Goodenough et al. (2010) noted that plutonic rocks belonging to the earliest phase of the Maevarano Suite in the Anaboriana Domain display a strong foliation at their margin and that the foliation mirrors the fabrics developed in the host rocks. Many of the Ambalavao Suite plutons exhibit the same structural relationship to regional fabrics that developed during thrusting or transpression in the older host

rocks. This indicates that magmatism, for the most part, post-dated the main crustal thickening event, but that some of the more pervasively foliated Ediacaran–Cambrian intrusions were emplaced late in the orogenic phase and consequently deformed only at their margins.

3.1. Ambalavao Suite

The Ambalavao Suite is named for the town of Ambalavao located approximately 50 km south of Fianarantsoa (BGS-USGS-GLW, 2008) and plutons are found throughout Madagascar (Roig et al., 2012; Tucker et al., 2012). The oldest age reported as being part of the Ambalavao Suite is 575 ± 16 Ma (BGS-USGS-GLW, 2008) while the Andringitra granite from Itremo region denotes the youngest pluton of 539 ± 2 Ma (Tucker et al., 2007). Texturally, intrusions are fine-grained equigranular to porphyritic and often pegmatitic (Table 1; Fig. 3). Compositionally, rocks are syenite, granite, granodiorite and gabbro (Fig. 4) with minor occurrences of anorthosite, orthopyroxenite and charnockite (BGS-USGS-GLW, 2008). Porphyritic and non-porphyritic granitoid intrusions are grouped into the Carion Subsuite (BGS-USGS-GLW, 2008). Vohombohitra Subsuite intrusions are found only in the northwest Antananarivo Domain (BGS-USGS-GLW, 2008).

Ambalavao Suite samples from this study belong to the Carion Subsuite including one sample of the Carion Pluton (Fig. 2). The subsuite is characterised by porphyritic syenogranite, quartz-syenite and granite with less abundant non-porphyritic granitoid plutons (BGS-USGS-GLW, 2008). Pegmatite dykes and/or pods are commonly associated with plutonic rocks (Fig. 3c). Weakly foliated granitoids often contain mafic enclaves and/or xenoliths of older lithologies. Peak metamorphism of host rocks in the Antananarivo Domain was dated at 546 ± 5 Ma (BGS-USGS-GLW, 2008) indicating that metamorphism and magmatism occurred simultaneously during the waning stages of late Neoproterozoic to lower Cambrian deformation. Many intrusions (including the Carion Pluton) show varying degrees of deformation from the margin to the interior of plutons (Collins et al., 2003a; Razanatseheno et al., 2009) and some plutons were locally deformed at their margins by E–W shortening either syn- or post-emplacement (Nédélec et al., 2000; Collins et al., 2003b; Razanatseheno et al., 2009).

3.2. Maevarano Suite

The Maevarano Suite is named after the Maevarano River where intrusions of the suite are best exposed in northern Madagascar (BGS-USGS-GLW, 2008). Batholiths and plutons are found mostly in the Anaboriana, the northern Antananarivo and the Bemarivo Domains (BGS-USGS-GLW, 2008; Goodenough et al., 2010; Zhou et al., 2015). Goodenough et al. (2010) subdivided the Maevarano Suite into three main magmatic phases based on whole-rock geochemistry and field relationships. The earliest magmatic pulses were the most mafic and foliated intrusions. Lithologies vary in composition from granodiorite, monzonite, and monzodiorite to diorite and gabbro (Fig. 4). Gabbroic intrusions are often associated with, and cross-cut by, younger intrusions of porphyritic granite of the second phase (Goodenough et al., 2010). The second main phase are typically porphyritic granitoids with microperthitic potassium feldspar phenocrysts up to 2.5 cm in diameter (Goodenough et al., 2010). There are also minor charnockite intrusions with up to 20 mol.% orthopyroxene (BGS-USGS-GLW, 2008; Goodenough et al., 2010). The youngest phase is characterised by medium-grained granitoids and pegmatite and aplite veins.

Based on field relationships alone, the Maevarano Suite samples under study could not be assigned to the magmatic phases proposed by Goodenough et al. (2010). However, U-Pb data indicate that the two samples of the Maevarano Suite (DA13-004 and DA13-006) belong to the earliest phase emplaced between ca. 537 Ma and 531 Ma (Goodenough et al., 2010).

Figure 3. Representative field photographs of the Ambalavao and Maevarano Suites. (a) Maevarano granite sample DA13-004; (b) foliated Ambalavao granite sample DA13-050; (c) pegmatite dyke crosscutting Ambalavao granite at the sampling location of sample DA13-010; (d) porphyritic granite sample DA14-128.

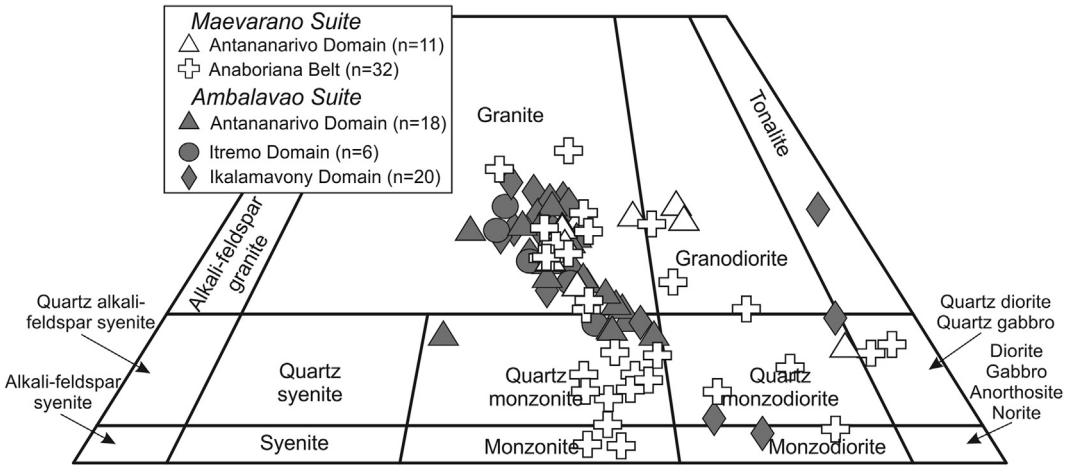

Figure 4. Quartz-Alkali-feldspar-Plagioclase (QAP) diagram for the Ambalavao and Maevarano Suites using the normative mineralogy calculated in IgPet. Data for the Ambalavao Suite are from this study, Meert et al. (2001a), BGS-USGS-GLW (2008) and CGS (2009). Data for the Maevarano Suite are from this study, Goodenough et al. (2010) and Zhou et al. (2015). Thirty Maevarano Suite samples were collected by BGS-USGS-GLW (2008) and published in Goodenough et al. (2010) and these samples have the same symbols on geochemical plots.

4. Analytical methods

A complete description of the analytical methods employed in this study is available in online supplementary Appendix A. Sample collection focused on obtaining representative samples including Ediacaran–Cambrian rocks from the Antananarivo, Itremo and Ikalamavony Domains (Fig. 2). Fourteen samples were selected for whole-rock geochemical analysis including two duplicate analyses (DA14-304 and DA14-372). Samples were analysed for major, minor and trace elements at ACME Labs in Vancouver, Canada. Major element data were collected using a SPECTRO AS500 ICP-OES (inductively coupled plasma optical emission spectrometry) instrument and trace element data were collected using a Perkin-Elmer ELAN 9000 solution ICP-MS (inductively coupled plasma mass spectrometry).

LA-ICP-MS (laser-ablation inductively coupled mass spectrometry) zircon U-Pb analyses were conducted at Adelaide Microscopy in Adelaide, Australia. Zircon standard reference material GJ (Jackson et al., 2004) was used as a primary standard and internal accuracy was monitored using the Plešovice zircon reference material ($^{206}Pb/^{238}U$ age of 337.1 ± 0.4 Ma, 2σ, Sláma et al., 2008). Plešovice analyses yield a weighted-mean $^{206}Pb/^{238}U$ age 338.2 ± 1.8 Ma (2σ, MSWD = 2.6; n = 63). Table 2 summarises the zircon morphologies and unknown sample U-Pb age deduction notes are listed in Table 3. Individual zircon U-Pb ages are quoted at the 1σ level and weighted-mean sample ages are at a 2σ level.

Zircon oxygen isotope analyses were conducted at the Australian National University, Canberra, Australia using the SHRIMP SI (sensitive high-resolution ion microprobe stable isotope) or SHRIMP II instrument. The SHRIMP SI method involved a 10 kV, ~3 nA Cs^+ primary ion beam focused to a ~30 μm in diameter spot size. Procedures for the SHRIMP II follow the methods of Ickert et al. (2008). Long term instrument drift was corrected using the Mudtank zircon reference material ($\delta^{18}O$ = 5.03‰ ± 0.10‰; Valley, 2003) and Temora II zircon ($\delta^{18}O$ = 8.20‰ ± 0.01‰; Valley et al., 2005). Standard results for each method are found in Appendix A (Table A1).

In situ LA-MC-ICP-MS (laser-ablation multi-collector inductively-coupled mass spectrometry) zircon Hf isotope analyses were conducted at the University of Adelaide, Waite Campus, facility using a New Wave Research 193 nm Excimer laser attached to a Neptune multi-collector ICP-MS system as per Payne et al. (2013). Analysis locations were in the same cathodoluminescence domains as concordant U-Pb laser spots and in the same site as SHRIMP oxygen isotope analysis locations (Fig. 5). Procedural accuracy was monitored using the Plešovice, Mudtank and Temora II zircon standards. Mean $^{176}Hf/^{177}Hf$ ratios for each standard along with the literature values are presented in Appendix A (Table A1). $\varepsilon_{Hf}(t)$ and T_{DM}^{c} were calculated using ^{176}Lu decay constant after Scherer et al. (2001). T_{DM}^{c} two stage crustal model ages were calculated using the methods of Griffin et al. (2002) with an average crustal composition of $^{176}Lu/^{177}Hf$ = 0.015.

5. Results

5.1. Sample descriptions and U-Pb zircon geochronology results

5.1.1. Ambalavao Suite

Sample DA13-010 was collected from a hillside exposure approximately 30 km north of Ambositra in the Antananarivo Domain (Table 1; Fig. 2). The pink, homogeneous granite is medium- to coarse-grained and undeformed. Coeval pegmatite leucosomes and lenses (cm to dm sized) are common (Fig. 3c) but contact relationships with older basement units are absent. The sample yielded a $^{206}Pb/^{238}U$ crystallisation age of 544 ± 5 Ma (Fig. 6a).

Sample DA13-018 was collected from a water-washed streambed exposure approximately 42 km west of Fianarantsoa in the Antananarivo Domain (Table 1; Fig. 2). The outcrop is massive and contact relationships with older units are absent but the Ambatolampy Group crops out 100 m northwest. Randomly oriented pegmatite and granite dykes (cm to dm sized) are also present. The sample of pink, homogeneous granite is fine-to medium-grained and undeformed. The sample has a $^{206}Pb/^{238}U$ crystallisation age of 580 ± 8 Ma (Fig. 6b).

Sample DA13-037 was collected from a hillside exposure approximately 55 km west of Fianarantsoa in the Antananarivo Domain (Table 1; Fig. 2). The outcrop contains small pegmatite dykes along with enclaves and xenoliths of older lithologies. The granite intruded intensely deformed and recrystallised quartzite and schist of the Ambatolampy Group (Archibald et al., 2015). The granite is fine- to medium-grained and displays variable foliation intensity on the outcrop scale. Syn-emplacement foliation variability represents strain partitioning within the granite. The sample has a $^{206}Pb/^{238}U$ crystallisation age of 549 ± 9 Ma (Fig. 6c).

Table 2
Physical and optical characteristics of zircon from the Ambalavao and Maevarano Suites.

Sample	Colour	Size (mm)	Aspect ratio (L:W)	Morphology	Internal zoning
DA13-004	clear, pale yellow	50–350	2:1 to 4:1	mostly euhedral to subhedral	xenocrystic cores; dark magmatic oscillatory zoning; some grains contain inclusions of unknown mineral
DA13-006	clear, pale yellow	100–400	2:1 to 5:1	mostly euhedral to subhedral	bright magmatic oscillatory zoning; some grains contain inclusions of unknown mineral
DA13-010	clear, colourless	50–250	2:1 to 4:1	mostly subhedral to euhedral	bright cores with magmatic oscillatory zoning; dark outer rims, dark inclusions
DA13-018	clear, colourless	50–250	1:1 to 3:1	mostly subhedral to euhedral	dark unzoned; faint magmatic oscillatory zoning
DA13-037	clear, pale brown	50–350	2:1 to 4:1	mostly subhedral	bright magmatic oscillatory zoning; narrow, dark overgrowths
DA13-038	clear, pale yellow	50–200	2:1 to 4:1	mostly subhedral	bright magmatic oscillatory zoning; narrow, dark overgrowths; some grains contain inclusions of unknown mineral
DA13-041	clear, colourless	50–300	1:1 to 4:1	mostly subhedral	bright, broad magmatic oscillatory zoning
DA13-050	colourless, clear	50–325	2:1 to 5:1	euhedral to subhedral	magmatic oscillatory zoning and narrow, dark coloured overgrowths
DA13-051	clear, pale yellow	50–325	2:1 to 5:1	euhedral to subhedral	small, dark core domains, bright magmatic oscillatory zoning, minor sector zoning
DA13-072	clear	100–400	2:1 to 3:1	mostly subhedral to euhedral	dark mineral inclusions; bright, unzoned domains, magmatic oscillatory zoning; some grains have irregular zoning and dark, narrow overgrowths
DA14-126	colourless, pale brown	150–600	2:1 to 4:1	mostly subhedral to euhedral	dark, unzoned cores; faint, bright, broadly zoned overgrowths; abundant cracks and inclusions
DA14-128	colourless, pale brown	75–500	1:1 to 3:1	mostly euhedral to subhedral	dark, unzoned cores; faint, bright, broadly zoned overgrowths; abundant cracks and inclusions

Sample DA13-038 was collected from a hillside outcrop approximately 52 km west of Fianarantsoa in the Antananarivo Domain (Table 1; Fig. 2). The outcrop contains many cm to dm sized pegmatite dykes and lenses. The fine- to medium-grained granite displays a variable foliation on the outcrop scale similar to sample DA13-037. Quartzite of the Ambatolampy Group is observed above the weakly foliated granite. The sample has a $^{206}Pb/^{238}U$ crystallisation age of 544 ± 7 Ma (Fig. 6d).

Sample DA13-041 was collected from a streambed outcrop approximately 48 km west of Fianarantsoa in the Antananarivo Domain (Table 1; Fig. 2). The sample was collected from an unaltered granite dyke (~50 cm in width) cross cutting weathered granite of the Imorona-Itsindro Suite. Other granite dykes, mafic dykes and pegmatite lenses are also present cross cutting the main Tonian-aged body. U-Pb (zircon) analyses showed no evidence of inheritance of Tonian-aged zircon (Fig. 6e). The sample has a $^{206}Pb/^{238}U$ crystallisation age of 550 ± 8 Ma (Fig. 6e).

Sample DA13-072 was collected from a roadside outcrop of the Carion Pluton approximately 25 km east of Antananarivo along RN2 in the Antananarivo Domain (Table 1; Fig. 2). The Carion Pluton is porphyritic syenogranite with amphibole, biotite, quartz, and alkali-feldspar phenocrysts. The matrix consists of fine-grained alkali-feldspar, quartz, plagioclase, amphibole, biotite, opaque minerals, opaque minerals, and zircon. The sample yielded a $^{206}Pb/^{238}U$ crystallisation age of 544 ± 4 Ma (Fig. 6f). Previous geochronological data from this pluton yielded a $^{207}Pb/^{206}Pb$ age of 537.6 ± 1.0 Ma (Kröner et al., 2000) and SHRIMP U-Pb ages of 532.1 ± 5.2 Ma (Meert et al., 2001b) and 540 ± 5 Ma (BGS-USGS-GLW, 2008). Here, we interpret the more recently obtained SHRIMP and LA-ICP-MS ages (ca. 544–540 Ma) to represent the early crystallization of parts of the Carion Pluton. The younger SHRIMP age (Meert et al., 2001a) may reflect younger crystallization of a composite intrusion and protracted emplacement over ca. 10–12 Myrs. The pluton is located near the Angavo-Ifandiana Shear zone (Fig. 2), a structure that provided a pathway for magma ascent that was active to ca. 530 Ma (Grégoire et al., 2009; Raharimahefa and Kusky, 2010).

Sample DA13-050 was collected from a hillside outcrop approximately 17 km south of Ambositra along RN 35 in the Itremo Domain (Table 1; Fig. 2). The granite contains biotite-rich mafic enclaves. The rock is weakly foliated and the flattened enclaves (cm-sized) define the foliation. The main granite body is massive, weakly foliated (Fig. 3b) with cross cutting pegmatite dykes (cm to dm sized). The sample has a $^{206}Pb/^{238}U$ crystallisation age of 570 ± 8 Ma (Fig. 7a).

Sample DA13-051 was collected from a hillside outcrop approximately 20 km south of Ambositra along RN 35 in the Itremo Domain (Table 1; Fig. 2). The granite body has a strong foliation and the outcrop displays abundant pegmatite dykes and pods (cm to dm sized). This sample is from the margin of a larger intrusion and that the foliation formed syn-emplacement. The sample yielded an imprecise $^{207}Pb/^{206}Pb$ crystallisation age of 581 ± 33 Ma (Fig. 7b).

Sample DA14-126 was collected from a small roadside quarry outcrop approximately 2 km east of Miandrivazo along RN34 in the Ikalamavony Domain (Table 1; Fig. 2). The porphyritic granite is observed in contact with highly weathered schist of the Ikalamavony Group (Fig. 8a). There is a small deformation zone in this outcrop that mirrors the regional structure of the Dabolava Shear Zone (CGS, 2009). The porphyritic granite becomes less deformed moving away from the contact zone into undeformed rocks. The deformation in the underlying schist mirrors the foliation observed in the granite. Other contact relationships with the underlying Ikalamavony Group (e.g. xenoliths) are not recognised indicating this is a thrust contact. Therefore, we interpret these structures as S-C fabrics developed during E–W (top to the west) thrusting of the granite pluton over the Ikalamavony Group. Thrusting occurred late-syn to early-post emplacement of the granite. Small (cm-scale) pegmatite dykes cross cut the granite, schist and the deformation zone (Fig. 8a). The medium-to coarse-grained porphyritic granite has phenocrysts (<1 cm) of quartz and alkali-feldspar. The sample yielded a $^{206}Pb/^{238}U$ age of 559 ± 10 Ma (Fig. 7c), an age that records the crystallization of the granite.

Sample DA14-128 was collected from a small roadside outcrop approximately 5 km east of Miandrivazo along RN34 in the Ikalamavony Domain (Table 1; Fig. 2). Contact relationships between the coarse-grained porphyritic granite and older units are not observed at this location (Fig. 3c). Compared to sample DA14-126, this porphyritic granite is undeformed. The sample contains

Table 3
Summary of U-Pb data and age deduction notes for samples of the Ambalavao and Maevarano Suites. Unless otherwise stated, concordant data refers to the ≥95% concordance level.

Sample	*n*	*n* (≥95%)	Pb_c (%)	Remarks	Age (Ma)
DA13-010 (Ant)	40	18	0.00–1.70	All concordant data yields a weighted-mean $^{206}Pb/^{238}U$ age of 547 ± 9 Ma (MSWD = 3.4; *n* = 18). Omitting the two oldest analyses (interpreted to represent inheritance) and one younger analysis (interpreted as Pb loss) that plot away from the main cluster yields a more precise and reliable $^{206}Pb/^{238}U$ age of 544 ± 5 Ma (MSWD = 0.82; *n* = 15). The data spread is attributed to common Pb and Pb-loss. One concordant analysis has an age of 775 ± 11 Ma is interpreted as inherited from the Imorona-Itsindro Suite, which crops out nearby.	544 ± 5
DA13-018 (Ant)	22	13	0.00–2.02	The data yield a relatively imprecise $^{206}Pb/^{238}U$ age of 579 ± 10 Ma (MSWD = 5.6; *n* = 13). One grain has a concordant $^{206}Pb/^{238}U$ age of 516 ± 8 Ma, but its significance is uncertain. The $^{207}Pb/^{206}Pb$ age for the same data is 662 ± 20 Ma (MSWD = 0.91; *n* = 14). Omitting the two oldest analyses (interpreted to represent inheritance) and two youngest analyses (interpreted as Pb loss domains) that plot away from the main data cluster yields a $^{206}Pb/^{238}U$ age of 580 ± 8 Ma (MSWD = 2.3; *n* = 9) that interpreted as the crystallisation age.	580 ± 8
DA13-037 (Ant)	22	6	0.00–1.12	The spread in concordant data is attributed to post-crystallisation Pb-loss. The weighted-mean $^{206}Pb/^{238}U$ age is 549 ± 9 Ma (MSWD = 1.2; *n* = 6) and is interpreted to best represent the crystallisation age.	549 ± 9
DA13-038 (Ant)	43	19	0.00–0.91	A $^{206}Pb/^{238}U$ age of 545 ± 11 Ma (MSWD = 7.0; *n* = 19) is calculated using only the concordant data. The $^{207}Pb/^{206}Pb$ age for the same data is 614 ± 27 Ma (MSWD = 0.67; *n*= 19). Omitting the two oldest (interpreted as inherited) and youngest ages (Pb loss) to improve age uncertainty and precision gives a $^{206}Pb/^{238}U$ age of 544 ± 7 Ma (MSWD = 2.3; *n* = 15), an age interpreted to best represent the crystallisation age.	544 ± 7
DA13-041 (Ant)	15	5	0.00–0.59	The weighted-mean $^{206}Pb/^{238}U$ age is 550 ± 8 Ma (MSWD = 0.43; *n* = 5), an age interpreted to most accurately represent the crystallisation age.	550 ± 8
DA13-072 (Ant)	29	28	0.00–1.24	The weighted-mean $^{206}Pb/^{238}U$ age is 544 ± 4 Ma (MSWD = 1.6; *n* = 28). The same data yield a less precise $^{207}Pb/^{206}Pb$ age of 546 ± 22 Ma (MSWD = 0.79; *n* = 28).	544 ± 4
DA13-050 (Itremo)	29	18	0.00–0.61	Concordant data plot as an array along concordia between ~525 Ma and ~620 Ma. The $^{206}Pb/^{238}U$ age weighted-average age is 568 ± 12 Ma (MSWD = 8.6; *n* = 18). The $^{207}Pb/^{206}Pb$ ratios for the same data yield an imprecise age of 583 ± 35 Ma (MSWD = 1.8; *n* = 18). Omitting the oldest and youngest ages that plot away from the main data cluster yields a more precise age of $^{206}Pb/^{238}U$ 570 ± 8 Ma (MSWD = 2.5; *n* = 14) that is interpreted best represent the crystallisation age.	570 ± 8
DA13-051 (Itremo)	43	30	0.00–3.58	The $^{206}Pb/^{238}U$ age is 542 ± 5 Ma (MSWD = 2.1; *n* = 30). The $^{207}Pb/^{206}Pb$ age for the same data is 581 ± 33 Ma (MSWD = 0.55; *n* = 30). Upper and lower intercepts for the same data are 582 ± 120 Ma and the origin (76 ± 1500 Ma). Although the $^{206}Pb/^{238}U$ age is more precise, the data spread implies the $^{207}Pb/^{206}Pb$ age of 581 ± 33 Ma is more representative of the crystallisation age.	581 ± 33
DA14-126 (Ikal)	28	10 (≥90%)	0.01–1.54	The ≥ 90% concordance is used because of the lack of ≥95% concordant grains. The $^{206}Pb/^{238}U$ age is 556 ± 10 Ma (MSWD = 4.6; *n* = 10). When one analysis is discarded, the remaining nine are within 5% of the concordia and yield a $^{206}Pb/^{238}U$ age of 559 ± 10 Ma (MSWD = 3.6; *n* = 9). The $^{207}Pb/^{206}Pb$ age for the same data yields an older, imprecise age of 629 ± 23 Ma (MSWD = 1.05; *n* = 10). The $^{206}Pb/^{238}U$ age of 559 ± 10 Ma is considered a better representation of the crystallisation age.	559 ± 10
DA14-128 (Ikal)	22	9 (≥90%)	0.01–0.71	The $^{206}Pb/^{238}U$ age calculated using the ≥90% concordant data yields an imprecise age of 538 ± 17 Ma (MSWD = 4.6; *n* = 9). The $^{206}Pb/^{238}U$ age calculated with the ≥95% concordant data is 553 ± 7 Ma (MSWD = 0.63; *n* = 4) but includes only four analyses. By omitting the youngest ≥90% concordant analysis that plots away from the main data cluster, a more reliable and precise $^{206}Pb/^{238}U$ age of 545 ± 7 Ma (MSWD = 1.7; *n* = 8) is obtained. This zircon likely experienced Pb loss and is justifiably omitted from the age calculation.	545 ± 7
DA13-004 Maevarano (Ant)	60	20	0.00–0.32	The weighted mean $^{206}Pb/^{238}U$ crystallisation age is 531 ± 6 Ma (MSWD = 2.9; *n* = 20). Two slightly older concordant grains yield U-Pb ages of 650 ± 8 Ma and 660 ± 8 Ma and are interpreted as inherited. Three older grains with Palaeoproterozoic crystallisation ages are also interpreted as inherited but are not shown on Fig. 7e.	531 ± 6
DA13-006 Maevarano (Ant)	57	36	0.00–1.65	The weighted mean $^{206}Pb/^{238}U$ age is 515 ± 8 Ma (MSWD = 7.6; *n* = 36). Using the "unmix" feature in Isoplot, there appears to be two separate age populations with $^{206}Pb/^{238}U$ ages of 535 ± 5 Ma (MSWD = 1.5; *n* = 22) and 495 ± 6 Ma (MSWD = 1.7; *n* = 14). CL images show no significant differences in zoning patterns between the older and younger populations. To visually distinguish between the two groups, the most discordant grains are not plotted on Fig. 7f but are included in Appendix A. Whether this data represents two meaningful ages or whether the spread is explained by a Pb-loss model is unclear. The weighted mean $^{207}Pb/^{206}Pb$ age for all concordant data is 567 ± 23 Ma (MSWD = 0.69; *n* = 36). The imprecision associated with the $^{207}Pb/^{206}Pb$ age and the indication of Pb loss implies that the $^{206}Pb/^{238}U$ age of 535 ± 5 Ma as the most representative crystallisation age.	535 ± 5

Abbreviations: Ant, Antananarivo Domain; Itremo, Itremo Domain; Ikal, Ikalamavony Domain.

phenocrysts (~1–2 cm) of quartz and alkali-feldspar. The sample yielded a $^{206}Pb/^{238}U$ age of 545 ± 7 Ma (Fig. 7d).

5.1.2. Maevarano Suite

Sample DA13-004 was collected from the Ambatolampy Quarry approximately 70 km south of Antananarivo in the Antananarivo Domain (Table 1; Fig. 2). The granite dyke intrudes into Betsiboka Suite orthogneiss in the Antananarivo Domain basement (D.B. Archibald unpublished $^{207}Pb/^{206}Pb$ age of 2507 ± 17 Ma) and undated dykes of the Imorona-Itsindro Suite. The granite is fine-grained, undeformed (Fig. 3a) and exposed as a series of small dykes (cm to dm sized). The sample yielded a $^{206}Pb/^{238}U$ crystallisation age of 531 ± 6 Ma (Fig. 7e).

Sample DA13-006 was collected from a small quarry approximately 2 km north of Ambositra in the Antananarivo Domain (Table 1; Fig. 2). Contact relationships with older units were not observed at this outcrop but coeval or younger pegmatite dykes (10 cm wide) and lenses containing black tourmaline are present. The dated granodiorite sample is medium- to coarse grained and undeformed except for discrete zones in the outcrop that have a minor foliation. The sample has a $^{206}Pb/^{238}U$ age of 535 ± 5 Ma (Fig. 7f).

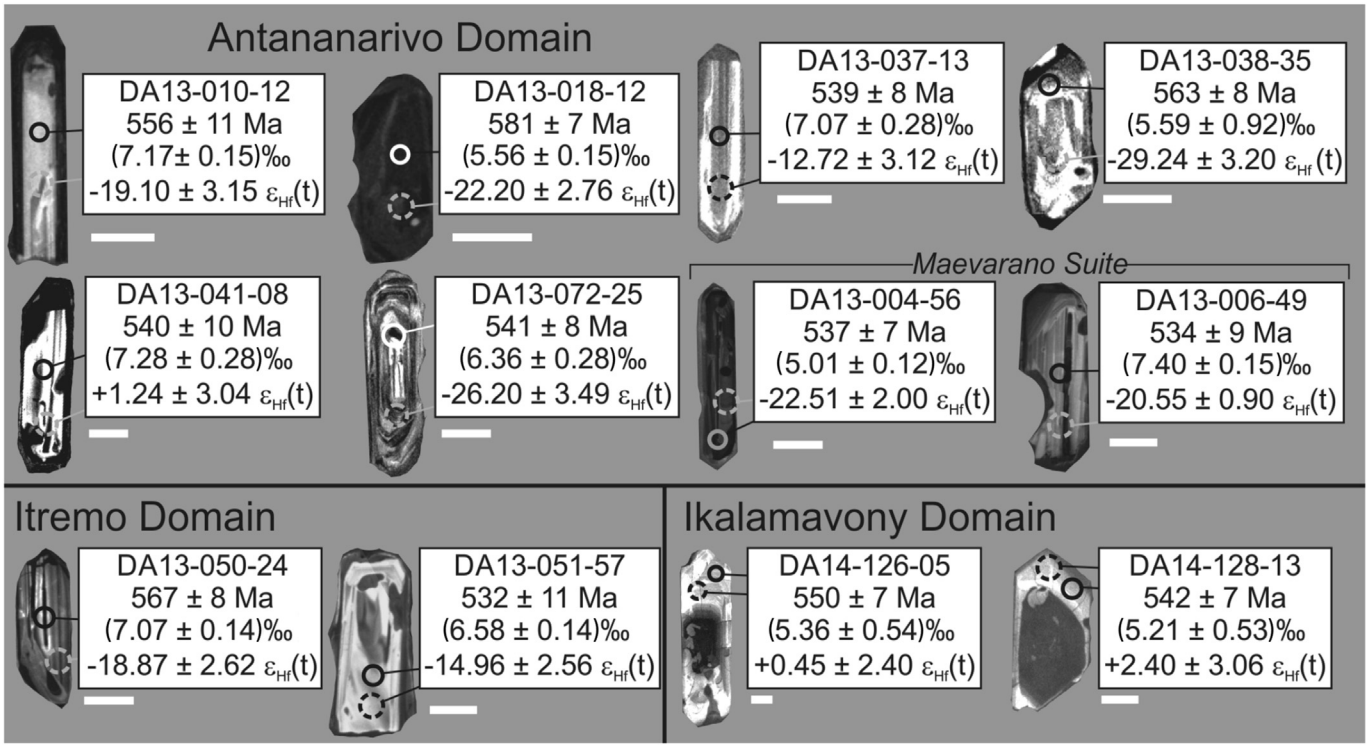

Figure 5. Cathodoluminescence (CL) images for representative zircon from the Ambalavao and Maevarano Suites. Analysis names, U-Pb ages with one standard deviation (s.d.) uncertainty, $\delta^{18}O$ values with two s.d. uncertainty and $\varepsilon_{Hf}(t)$ values with two s.d. uncertainty are listed beside each image. Solid circles represent U-Pb analysis spots and broken circles indicate the location of oxygen and hafnium isotope analyses. Scale bars beside each image are 50 μm.

5.2. Whole-rock geochemistry

Silica compositions are highly variable between 46.98 wt.% and 76.45 wt.% in Ambalavao Suite samples (Fig. 9). Most samples have low TiO_2 concentrations (<3 wt.%; Fig. 9a) and $Fe_2O_3^T$ (=FeO + Fe_2O_3) contents are between 0.94 wt.% and 11.85 wt.% (Fig. 9b). With the exception of the most mafic samples, MgO concentrations are also low (<3 wt.%; Fig. 9c) and CaO contents range from 0.31 wt.% for the most silica rich sample to 13.49 wt.% for a gabbroic sample (Fig. 9d). All four of these major element oxides show a strong negative correlation with increasing silica (Fig. 9). K_2O (0.41–10.50 wt.%) and Na_2O (1.30–5.25 wt.%) concentrations are variable across different SiO_2 compositions but both elements have a weak positive correlation with SiO_2 (Fig. 9e and f). Al_2O_3 contents (12.08–18.67 wt.%) do not correlate with SiO_2 concentrations (Fig. 9g). MnO (0.01–0.21 wt.%) and P_2O_5 (0.02–1.07 wt.%) concentrations are low and both oxides show a negative correlation with increasing SiO_2 (Fig. 9h and i).

Silica contents for Maevarano Suite samples are between 45.40 wt.% and 78.25 wt.% (Fig. 9). Most samples are low in TiO_2 (<3 wt.%) and have negative correlations with increasing silica (Fig. 9a). $Fe_2O_3^T$ concentrations are slightly higher than the Ambalavao Suite samples between 1.14 wt.% and 13.69 wt.% (Fig. 9b). MgO contents are low (<3 wt.%) but the seven samples with the lowest SiO_2 have higher MgO concentrations >3 wt.% (Fig. 9c). CaO contents range from 0.05 wt.% for the most silica rich sample to 10.68 wt.% for a gabbroic sample (Fig. 9d). K_2O (0.21–6.38 wt.%) and Na_2O (0.05–6.77 wt.%) concentrations are variable across increasing silica contents but both alkali elements have broad positive correlation with SiO_2 (Fig. 9e and f). Al_2O_3 contents vary (10.13–19.58 wt.%) and intermediate rocks have the highest concentrations (Fig. 9g). MnO (0.01–0.23 wt.%) and P_2O_5 (0.02–1.38 wt.%) contents are invariably low and both element oxides show a weak negative correlation with increasing SiO_2, especially at higher SiO_2 concentrations >60 wt.% (Fig. 9h and i).

Chondrite-normalised rare-earth element (REE) diagrams show a pronounced negative LREE and a flat HREE profile (Fig. 10a). All samples have negative Eu anomalies ($Eu/Eu^* = 0.51–0.78$; Fig. 10a; Table 4) implying a role for plagioclase fractionation. Some samples from previous studies have more pronounced negative anomalies (Eu/Eu^* as low as 0.28; CGS, 2009) in felsic samples and positive anomalies (Eu/Eu^* up to 3.22; CGS, 2009) in more mafic samples. Major, minor or trace element characteristics for Ambalavao Suite samples are consistent across all lithotectonic domains in central Madagascar (Fig. 10a–f). Ambalavao Suite samples have enrichment in the large-ion-lithophile elements (LILEs) and all samples show negative Ta-Nb, P, and Ti anomalies but the extent of each anomaly is variable (Fig. 10a).

Trace element patterns for the Maevarano Suite mirror those of the Ambalavao Suite (Fig. 10). Maevarano Suite samples exhibit a moderately steep negative LREE profile and a flat HREE profile (Fig. 10g). Eu/Eu^* ratios for Maevarano Suite granitoid samples are between 0.55 and 0.61 (Fig. 10g; Table 4), but Eu/Eu^* values are between 0.15 and 2.91 for all Maevarano Suite samples (Goodenough et al., 2010). Total REE concentrations are higher in samples collected from the Antananarivo Domain than in the Anaboriana Domain (Fig. 10g). Samples show enrichment in LILEs and negative Ta-Nb, P, and Ti anomalies (Fig. 10h).

Ambalavao Suite granitoids typically have elevated concentrations of total alkalis, Ga/Al ratios, high-field strength elements (HFSE), total REE with lesser amounts of CaO, MgO, Sr, Ni and Cr. Most samples display moderately negative Eu anomalies suggesting plagioclase fractionation. However, some of the gabbroic and charnockite samples show positive Eu anomalies indicating plagioclase accumulation. Most granitoid samples are ferroan (Fig. 11a) and metaluminous to peraluminous (Fig. 11b). Samples typically have

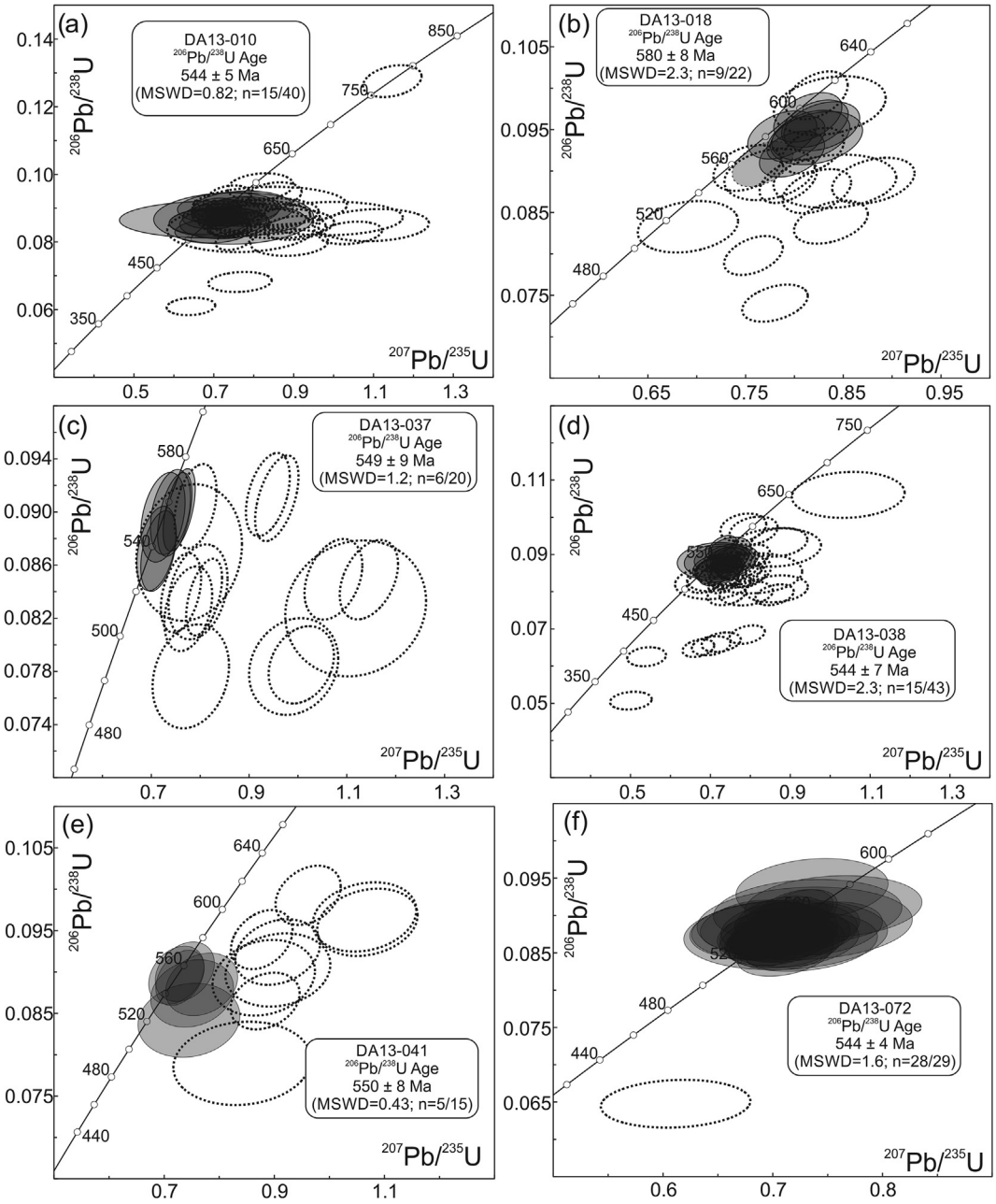

Figure 6. Concordia diagrams showing zircon analyses from the Ambalavao Suite collected from the Antananarivo Domain: (a) DA13-010; (b) DA13-018; (c) DA13-037; (d) DA13-038; (e) DA13-041; (f) DA13-072. U-Pb data are reported in Appendix A. Data point error ellipses are 2σ. Shaded ellipses were used in the weighted-mean age calculation and open ellipses were rejected.

high Ga/Al ratios and Zr concentrations (Fig. 11c). Further classification shows that samples are A2 type granitoids (Eby, 1992) although most samples plot near the dividing line (Fig. 11d). On tectonic discrimination diagrams, samples plot near the boundary between the within-plate granite and volcanic-arc granite fields (Fig. 10 e, f) in the post-collisional granite field (Pearce, 1996).

Maevarano Suite granitoid samples have enrichment in LILEs, LREEs and moderately negative Eu anomalies. Samples are ferroan (Fig. 11a) and mostly metaluminous to slightly peraluminous (Fig. 11b) with elevated Ga/Al ratios and high Zr concentrations (Fig. 11c). Most samples have Y/Nb ratios greater than 1.2 and plot in the A2 granite field (Eby, 1992; Fig. 11d). On tectonic discrimination diagrams Maevarano Suite samples plot in the post-collisional (Fig. 11e) and within-plate granite fields (Fig. 11f).

5.3. Oxygen isotopes

Oxygen isotope data were collected from zircon in ten samples of the Ambalavao Suite from the Antananarivo, Itremo and Ikalamavony domains in central Madagascar (Fig. 2). In six samples collected in the Antananarivo Domain, $\delta^{18}O$ values are between 5.56‰ ± 0.71‰ and 7.03‰ ± 0.89‰ (Fig. 12a). The mean $\delta^{18}O$ value for all six samples is 6.32‰ ± 1.52‰ ($n = 54$ zircon analysed). Five individual analyses of zircon from the Antananarivo Domain had outlier $\delta^{18}O$ values less than 5.0‰ (Appendix C) are not included in the above mean $\delta^{18}O$ calculation. Lower $\delta^{18}O$ values (<5.3‰ ± 0.6‰) represent high-T interactions of meteoric water with evolving magmas (Bindeman, 2008). The zircon grains with anomalously low $\delta^{18}O$ values are interpreted to be partially

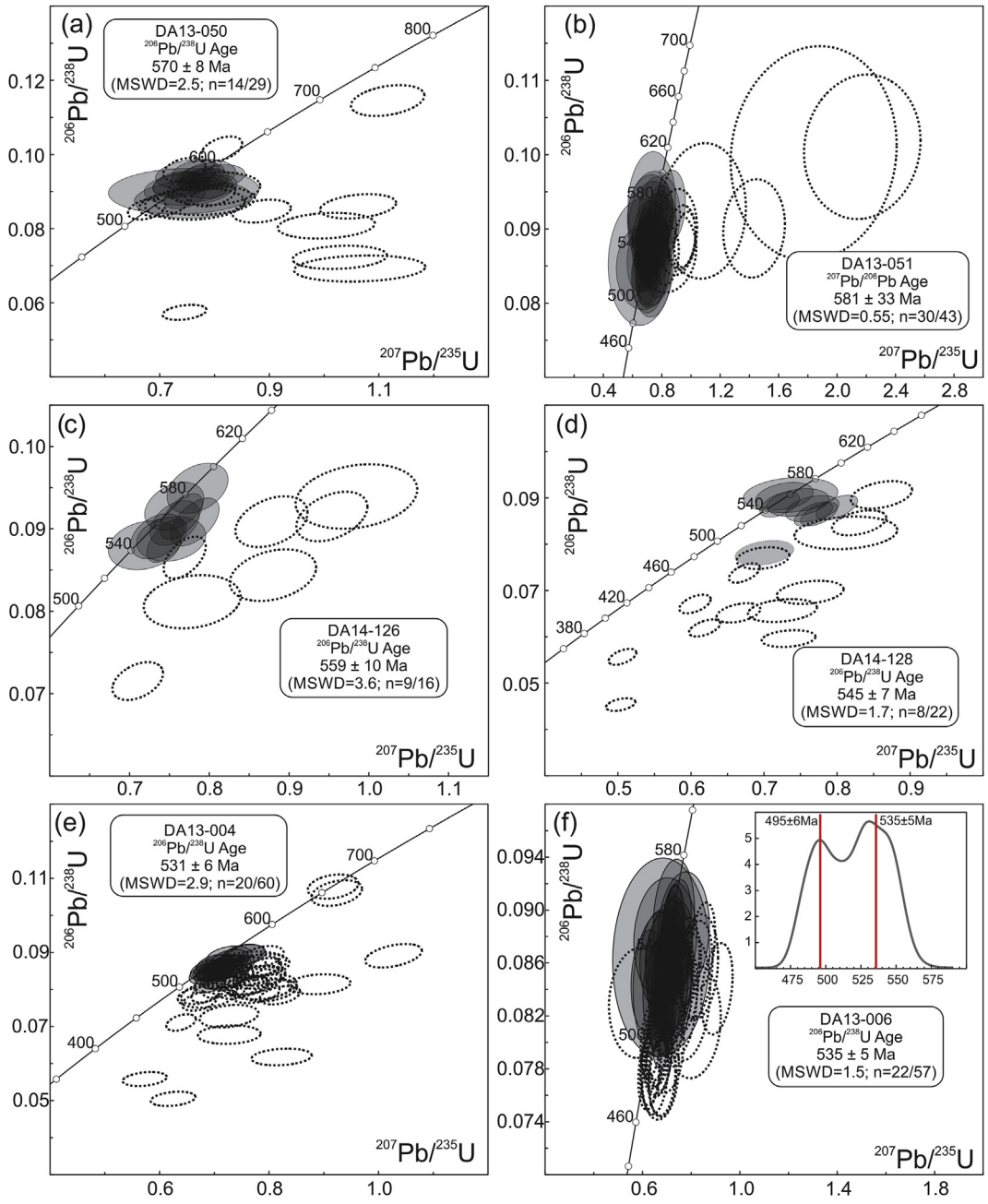

Figure 7. Concordia diagrams showing zircon analyses collected from samples of the Ambalavao Suite intruding the Itremo and Ikalamavony Domains and the Maevarano Suite in the Antananarivo Domain. (a) DA13-050; (b) DA13-051; (c) DA14-126; (d) DA14-128; (e) DA13-004; (f) DA13-006. U-Pb data are reported in Appendix A. Data point error ellipses are 2σ. Shaded ellipses were used in the weighted mean age calculation and open ellipses were rejected.

inherited from the Imorona-Itsindro Suite intrusions where lower zircon $\delta^{18}O$ values are more common (Archibald et al., 2016). Two samples from the Itremo Domain have average $\delta^{18}O$ values of 7.45‰ ± 0.68‰ and 6.58‰ ± 0.63‰. Ikalamavony Domain samples have lower $\delta^{18}O$ values of 5.32‰ ± 0.58‰ and 5.27‰ ± 0.72‰ (mean = 5.30‰ ± 0.64‰; $n = 16$) that plot within the mantle range (Fig. 12a). One zircon grain from sample DA14-126 has a lower $\delta^{18}O$ value (Appendix C) and is interpreted as inherited.

Oxygen isotope data were collected from zircon in two samples of the Maevarano Suite (Fig. 12a). Twelve analyses on two samples of the Maevarano Suite yielded mean $\delta^{18}O$ values of 5.58‰ ± 1.4‰ (DA13-004; 2σ; $n = 6$) and 7.28‰ ± 0.76‰ (DA13-006; 2σ; $n = 6$).

5.4. Hafnium isotopes

Fifty-five analyses from the same six samples of the Ambalavao Suite intruding the Antananarivo Domain demonstrate a wide range in zircon $^{176}Hf/^{177}Hf$ ratios (Fig. 12b). Age corrected mean $\varepsilon_{Hf}(t)$ values for individual zircon grains are between −27.8 ± 2.6 and −2.7 ± 6.6 (Appendix D) with corresponding T_{DM}^{c} model ages between 3.2 ± 0.2 Ga and 1.7 ± 0.4 Ga. Sample DA13-041 had only three zircons analysed for Hf isotopes and the ratios varied significantly (Appendix C). The remaining samples exhibit a narrower range of $\varepsilon_{Hf}(t)$ values between −27.8 ± 2.6 and −12.3 ± 1.3 (Fig. 12b). Twelve analyses of Ediacaran zircon in two samples from the Itremo Domain

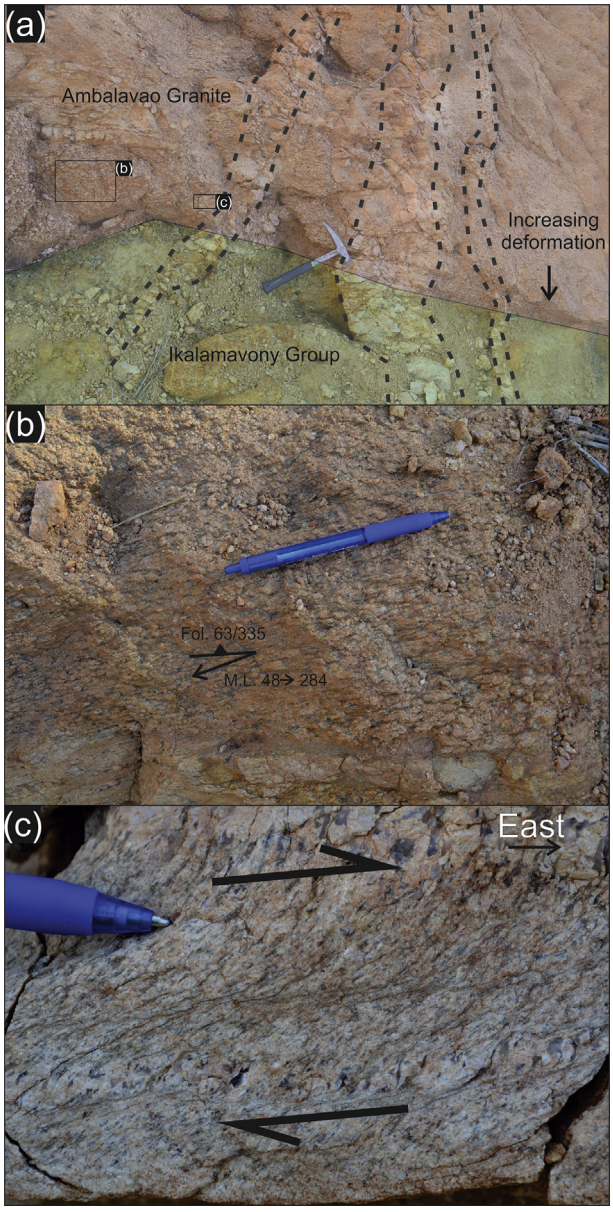

Figure 8. Field photographs of the sampling location of DA14-126. (a) Outcrop photograph showing the contact relationships between the Ambalavao Suite (pink), the Ikalamavony Group (green) and younger pegmatite dykes (outlined by broken lines); (b) strained granite near the contact zone; (c) S-C fabric in granite showing top-to-the-west deformation near the contact with the Ikalamavony Group.

have mean $\varepsilon_{Hf}(t)$ values of −19.7 ± 1.2 and −14.4 ± 2.6 (Fig. 10b). Corresponding T_{DM}^{c} model ages are 2.7 ± 0.1 Ga and 2.4 ± 0.2 Ga. Ediacaran zircon from the Ikalamavony Domain have more mantle-like $\varepsilon_{Hf}(t)$ signatures (Fig. 12b). Thirteen analyses from two samples have mean $\varepsilon_{Hf}(t)$ values of 0.0 ± 3.3 (DA14-126; 2σ; n = 7) and 0.2 ± 4.6 (DA14-128; 2σ; n = 6). Individual analyses in these two samples have larger 1σ uncertainties than zircon grains analysed from the other samples that are attributed to higher overall REE concentrations. This creates additional uncertainty due to the extent of the ^{176}Yb interference on ^{176}Hf measurements (Appendix D). Shorter analysis time due to the slender nature of the analysed zircon grains after mounting and polishing also contributed to the higher uncertainty. Corresponding T_{DM}^{c} model ages are 1.5 ± 0.2 Ga.

Thirteen analyses on two samples of the Maevarano Suite yielded age-corrected mean zircon $\varepsilon_{Hf}(t)$ values of −22.1 ± 1.3 (DA13-004; 2σ; n = 7) and −21.0 ± 1.1 (DA13-006; 2σ; n = 6). Corresponding T_{DM}^{c} model ages are ca. 2.8 ± 0.1 Ga.

6. Discussion

6.1. Age of the Ambalavao and Maevarano Suites

The Ambalavao Suite intruded into the Antananarivo, Itremo, Ikalamavony, Bemarivo, and the southern Madagascar Domains between ca. 580 Ma and 540 Ma (Fig. 13). Maevarano Suite (ca. 537–522 Ma) plutons were emplaced mostly into the northern Antananarivo, Bemarivo and Anaboriana Domains (Goodenough et al., 2010) but plutons with U-Pb crystallisation ages younger than 540 Ma are found throughout Madagascar (Tucker et al., 2014). Magmatism was apparently constant over this time interval (ca. 580–520 Ma) but periods of increased magmatic activity are discernible (Fig. 13). The Ambalavao Suite (ca. 571 Ma, ca. 552 Ma, and ca. 541 Ma) pulses are widespread across all Precambrian domains. The ca. 529 Ma pulse corresponds to the main phase and the ca. 522 Ma pulse corresponds to the youngest phase of Maevarano Suite magmatism in the Anaboriana Domain (see spatial distribution in Fig. 15 in Tucker et al., 2014).

Magmatism is interpreted as being related to regional deformational events in central Madagascar that were associated with the amalgamation of Gondwana. D1 occurred prior to intrusion of the Ambalavao Suite and is a WSW-directed flat-lying foliation attributed to ca. 630 Ma extension (Nédélec et al., 2000) that manifested as an extensional detachment (Betsileo Shear Zone; Fig. 1b). This extensional event was syn-to post-collisional and interpreted to link central Madagascar (Azania) with East Africa in Gondwana before ca. 650 Ma (Collins et al., 2000). A more recent structural and geochronological study (Nédélec et al., 2016) posited that the major D1 extensional event occurred earlier during Tonian time (ca. 790–780 Ma). In either case, D1 pre-dates the intrusion of both the Ambalavao and Maevarano Suites.

Emplacement of the Ambalavao Suite coincided with the main phase of the Malagasy Orogeny (D2) between ca. 560 Ma and 530 Ma (Nédélec et al., 2000; Grégoire et al., 2009). D2 corresponds to a major E–W transpressive flexural zone that developed between ca. 630 Ma and 560 Ma (Nédélec et al., 2000). Grégoire et al. (2009) suggested transcurrent movement along the Angavo-Ifandiana Shear Zone (Fig. 2) was related to the D2 deformation and that a U-Pb monazite age of 550 ± 11 Ma dated the event. This shear zone developed during E–W compression (Martelat et al., 2000) and was identified as a pathway for magma ascent and enhanced fluid flow up to 60 km from the main shear zone between ca. 560–530 Ma (Raharimahefa and Kusky, 2010) that persisted until ca. 515 Ma (Grégoire et al., 2009). Emplacement of the earliest phase of the Maevarano Suite magmatism (Goodenough et al., 2010) overlaps with the latter stages of high-grade metamorphism in north Madagascar between ca. 560 Ma and 530 Ma (Jöns et al., 2009). Younger Maevarano Suite plutons were emplaced during the waning stages of Gondwana assembly during late-syn- or post-D2 deformation (Grégoire et al., 2009) or during a separate, D3 event due to continued movement along the Angavo-Ifandiana Shear Zone (Nédélec et al., 2000).

In the Ikalamavony Domain, Ambalavao Suite granite crosscuts the penetrative regional S1 fabric that developed after the main D1 orogenic episode (ca. 620 Ma; CGS, 2009). The Dabolava Shear Zone (Fig. 2) was interpreted as an accommodation structure (northwest-southeast trending sinistral shearing) associated with major sub-horizontal folding and thrusting during the main phase (D2; ca. 550 Ma) of deformation in western Madagascar (CGS, 2009).

D2 (and D3) deformation occurred during the main phase (ca. 560–530 Ma) of the Kuunga/Malagasy Orogeny in central

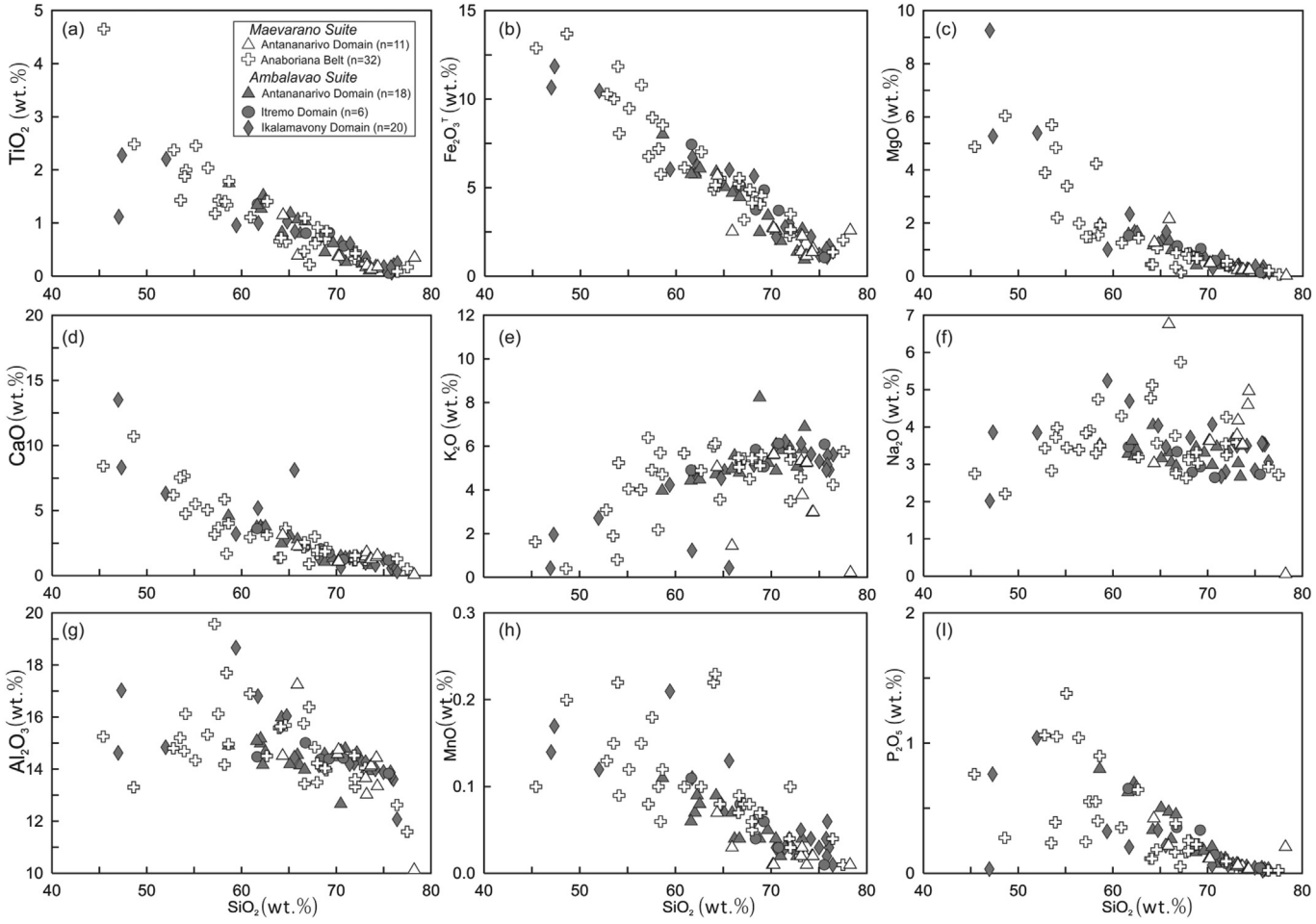

Figure 9. Harker major element variation diagrams for major element oxides, showing the extent to which Ambalavao and Maevarano Suite samples are fractionated and the degree of compositional overlap between the two suites. Data are from this study and the references listed in Fig. 4.

Madagascar (Meert, 2003). The Kuunga/Malagasy Orogeny (also known as the Pinjarra-Prydz-Denman Orogeny; Fitzsimons, 2003), closely followed the EAO marking the final major amalgamation of continental crust into Gondwana (Fig. 1a) with the suturing of Australia-East Antarctica against India and Kalahari and the wedging of Azania between India and the Congo-Tanzania-Bangweulu Block (Merdith et al., 2017). The association of ductile shear zones, regional metamorphism and late syn- to post-collisional magmatism is common throughout the EAO (Jacobs et al., 2008; Viola et al., 2008; Bingen et al., 2009). Magmatic suites with a similar emplacement age to the Ambalavao and Maevarano suites are found throughout the EAO (Fig. 1b) in East Antarctica (Jacobs et al., 2008; Elburg et al., 2016), Ethiopia (Blades et al., 2015, 2017), Mozambique (Jacobs et al., 2008; Bingen et al., 2009), Sudan and Somalia (Küster and Harms, 1998), Israel and Egypt (Be'eri-Shlevin et al., 2009), Namibia (Schmitt et al., 2012), Saudi Arabia (Robinson et al., 2014), and southern India (Plavsa et al., 2015). Many of these syn- to post-collisional granitoid suites are associated both spatially and temporally with major shear zone systems. Such shear zones include, for example, the Lurio Belt in Mozambique (Bingen et al., 2009), the "Main Shear Zone" in the Sør Rondane Mountains (Dronning Maud Land; Elburg et al., 2016), the Tulu Dimtu suture in Ethiopia (Blades et al., 2015, 2017), and the Palghat-Cauvery shear zone in Southern India (Plavsa et al., 2015).

Despite strong indications of crustal involvement from the hafnium isotopic data (discussed in section 6.3), there is little evidence for inheritance of older zircon (Appendix B; Figs. 6 and 7). Goodenough et al. (2010) also noted the lack of xenocrystic zircon domains in the Maevarano Suite. This differs from the zircon found in the Tonian-aged Imorona-Itsindro Suite that often preserve inherited domains, especially in samples that intruded the Antananarivo and Itremo domains (Archibald et al., 2016). The paucity of inherited ages implies high-temperature magmatism above the zircon saturation temperature. Alternatively, the source may not have contained Zr bearing minerals or Zr was part of another accessory phase such as baddeleyite. However, this explanation is considered unlikely given the abundance of zircon found in the rocks (e.g. Ambatolampy Group, Itremo Group, Imorona-Itsindro Suite, Betsiboka Suite, Ikalamavony Group and Dabolava Suite) that the Ambalavao and Maevarano Suites intruded (Tucker et al., 1999; Kröner et al., 2000; Cox et al., 2004; BGS-USGS-GLW, 2008; CGS, 2009; Tucker et al., 2012; Tucker et al., 2014; Archibald et al., 2015, 2016, 2018).

6.2. Petrogenesis of the Ambalavao and Maevarano Suites

The Maevarano Suite has geochemical characteristics that are indistinguishable from the Ambalavao Suite (Figs. 9–11) that are common in anorogenic or A-type granite suites (Whalen et al., 1987; Frost et al., 2001). The origin of metaluminous to peraluminous ferroan granitoids is considered differentiation of a tholeiitic basalt, low pressure melting of the crust and crustal

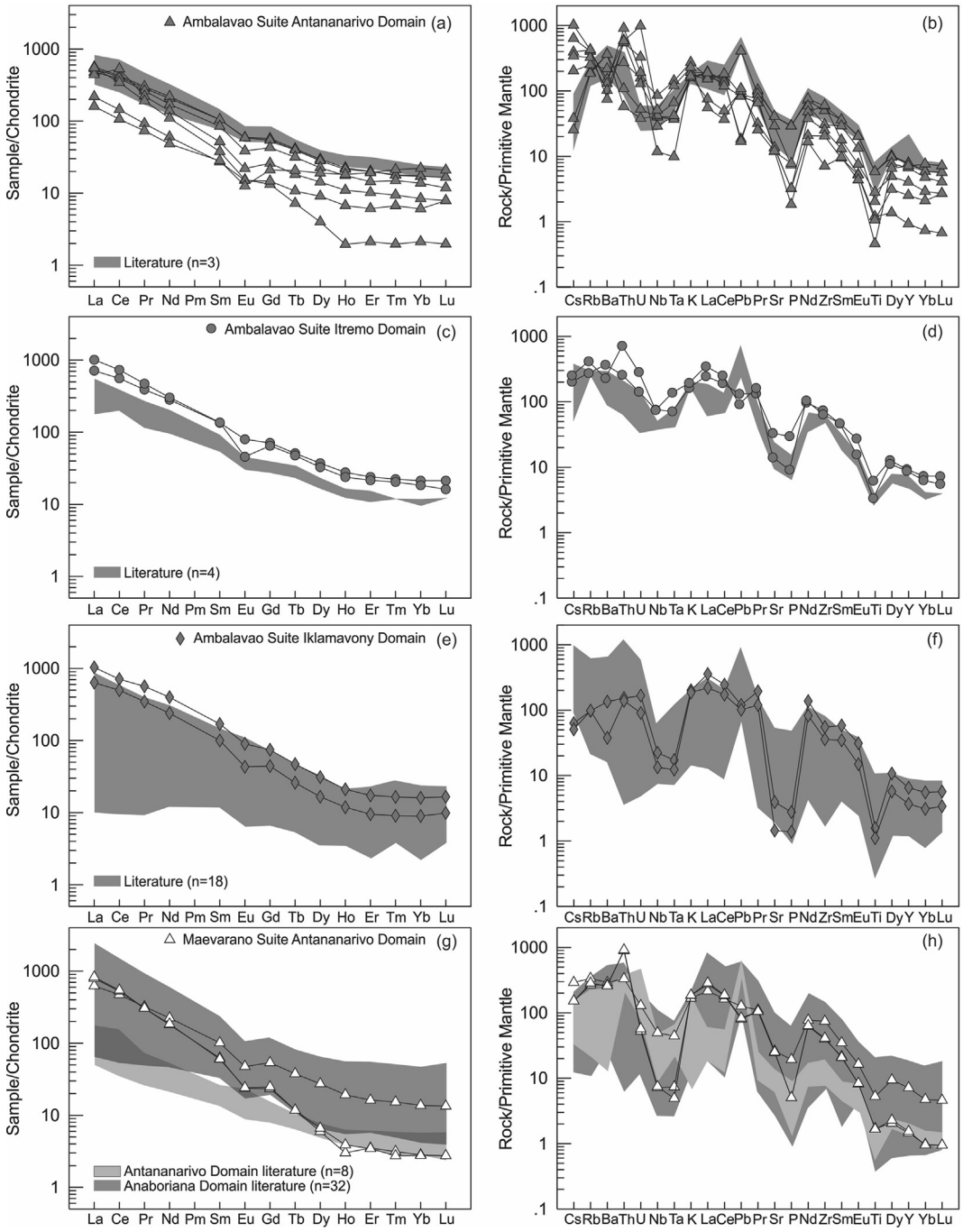

Figure 10. Chondrite-normalized REE diagrams and primitive mantle normalised trace-element spider diagrams for samples of the Ambalavao Suite intruding into the Antananarivo Domain (a–b), Itremo Domain (c–d), and Ikalamavony Domain (e–f) and Maevarano Suite samples from the Antananarivo Domain (g–h). Shaded fields show the range of REE and trace-element concentrations for literature data from the references listed in Fig. 4. Chondrite and primitive mantle values are from Sun and McDonough (1989).

assimilation (Turner et al., 1992; Frost and Frost, 2010). A1 type granite represents differentiates of magmas derived from sources similar to oceanic-island basalts but emplaced in continental rifts or during intraplate magmatism and A2 granite signifies magmas derived from continental crust or underplated crust that has been through a cycle of continent-continent collision or island-arc magmatism (Eby, 1992) and reflects the different sources involved during magma genesis (Pearce, 1996). Maevarano Suite samples are mostly A2 granites suggesting melt derivation from continental crust or underplated crust that experienced a cycle of continent-continent collision. We note, however, that many samples plot along the A1 and A2 fields dividing line.

Though most geochemical characteristics for the Ambalavao Suite are attributed to a syn- to post-collisional or an anorogenic tectonic setting, some geochemical traits observed are contradictory. Goodenough et al. (2010) noted that some of the geochemical trends in the Maevarano Suite are also inconsistent with an anorogenic setting. For example, geochemical attributes such as negative Ta-Nb, P, and Ti anomalies are often considered volcanic arc signatures (e.g., Murphy, 2007). We interpret these contradictory geochemical signatures to result from assimilation of the basement lithologies that these Ediacaran–Cambrian magmas intruded. Arc-magmatic rocks are a significant component of the Precambrian basement (Roig et al., 2012; Tucker et al., 2012). These

Table 4
Major (in wt.%) and trace element (in ppm) geochemical data collected in this study from the Ambalavao and Maevarano Suites.

	Maevarano Suite			Ambalavao Suite										
	DA13-004	DA13-006	DA14-304	DA13-018	DA13-031	DA13-037	DA13-038	DA13-041	DA13-050	DA13-051	DA13-072	DA14-126	DA14-128	DA14-372
SiO_2	70.26	64.35	70.16	70.97	73.47	72.71	69.65	68.78	68.37	61.65	62.02	70.50	76.45	62.02
Al_2O_3	14.75	14.52	14.58	14.79	13.93	14.30	14.46	14.58	14.39	14.48	14.99	14.70	12.08	15.18
$Fe_2O_3^T$	2.69	5.68	2.73	1.99	0.94	1.38	3.41	2.49	3.75	7.44	5.84	2.21	1.39	5.74
MgO	0.48	1.26	0.48	0.40	0.12	0.30	0.71	0.40	0.76	1.52	1.54	0.31	0.15	1.52
CaO	1.06	3.10	1.03	1.38	0.78	1.38	1.31	1.04	2.05	3.60	3.76	0.65	0.31	3.75
Na_2O	3.63	3.03	3.63	3.47	2.67	3.67	3.31	3.45	2.79	3.47	3.63	4.07	3.06	3.61
K_2O	5.61	5.04	5.58	5.81	6.87	5.05	5.23	8.22	5.84	4.90	4.78	6.06	5.61	4.80
TiO_2	0.36	1.14	0.37	0.26	0.10	0.23	0.61	0.44	0.73	1.35	1.26	0.34	0.24	1.26
P_2O_5	0.11	0.42	0.11	0.07	0.04	0.07	0.17	0.16	0.20	0.65	0.64	0.06	0.03	0.63
MnO	0.01	0.07	0.01	0.02	0.02	0.02	0.05	0.04	0.04	0.11	0.07	0.03	0.01	0.07
LOI	0.6	0.8	0.8	0.6	0.9	0.7	0.7	0.0	0.6	0.2	0.9	0.7	0.5	0.8
Total	99.54	99.45	99.54	99.72	99.82	99.80	99.64	99.60	99.51	99.36	99.41	99.66	99.81	99.39
Ba	1805	2031	1869	905	521	710	1049	1517	1610	2571	2535	941	263	2528
Be	<1	2	3	3	8	3	5	1	3	<1	3	<1	<1	1
Co	45	40	42	41	50	22	41	35	27	24	31	29	35	31
Cs	1	2	1	3	8	3	5	2	2	2	0	1	0	0
Ga	17	22	16	19	20	21	21	21	21	23	21	19	16	19
Hf	11	18	11	7	3	6	16	9	16	18	13	14	9	15
Nb	5	35	5	8	36	21	30	61	53	54	29	16	10	29
Rb	181	214	170	270	270	206	257	160	264	174	123	62	62	118
Sn	<1	4	<1	<1	3	1	3	3	3	4	3	1	<1	4
Sr	529	550	518	282	254	288	250	614	298	700	861	83	30	860
Ta	0	2	0	0	5	2	3	6	6	3	2	1	1	2
Th	78	28	76	77	49	46	51	23	61	22	5	13	12	9
U	1	3	1	4	21	7	3	3	6	3	1	4	2	1
V	19	59	18	15	<8	11	35	19	31	57	69	<8	<8	67
W	297	237	309	279	353	150	264	219	185	113	132	205	268	123
Zr	458	831	441	281	79	229	671	343	719	828	560	614	400	658
Y	7	32	7	4	32	12	18	30	40	42	36	30	17	36
La	196.1	148.0	188.6	130.0	37.8	51.6	104.4	112.5	239.0	168.7	126.6	245.1	150.4	133.8
Ce	332.8	288.8	322.9	210.2	64.9	88.1	323.4	239.3	447.7	341.5	250.1	434.6	305.2	261.2
Pr	29.1	30.5	28.9	18.1	7.0	8.8	21.1	25.0	44.7	37.0	27.0	53.6	33.0	28.6
Nd	86.2	104.5	84.5	51.2	22.5	28.1	64.7	79.8	141.4	131.3	96.1	186.0	111.7	102.5
Sm	9.2	15.5	9.5	5.8	4.3	4.2	7.9	12.9	20.8	20.6	16.0	25.9	15.3	16.1
Eu	1.4	2.8	1.4	0.9	0.7	0.9	1.3	2.2	2.7	4.6	3.4	5.2	2.5	3.4
Gd	5.1	11.0	4.8	2.7	4.3	3.0	5.3	8.8	13.3	14.6	11.8	15.3	9.1	11.1
Tb	0.4	1.4	0.4	0.3	0.8	0.4	0.7	1.2	1.8	1.9	1.5	1.8	1.0	1.5
Dy	1.7	6.9	1.5	1.0	4.8	2.3	3.6	5.7	8.3	9.5	7.5	7.9	4.2	7.1
Ho	0.2	1.1	0.2	0.1	1.0	0.4	0.6	1.0	1.4	1.6	1.3	1.2	0.7	1.2
Er	0.6	2.7	0.6	0.4	3.2	1.0	1.7	2.4	3.6	4.0	3.3	2.9	1.6	3.3
Tm	0.1	0.4	0.1	0.1	0.5	0.2	0.2	0.4	0.5	0.6	0.5	0.4	0.2	0.5
Yb	0.5	2.3	0.5	0.4	3.8	1.0	1.4	2.3	3.1	3.6	2.9	2.7	1.5	2.9
Lu	0.1	0.3	0.1	0.1	0.5	0.2	0.2	0.3	0.4	0.5	0.4	0.4	0.3	0.4
Mo	0	1	0	3	<0.1	0	1	1	1	1	1	1	0	1
Cu	21	14	19	2	1	2	10	12	7	8	14	2	4	13
Pb	6	9	6	6	8	7	6	29	7	9	1	9	7	1
Zn	37	98	35	27	7	15	55	10	73	131	58	58	35	58
Ni	2	6	2	1	1	1	3	2	2	1	8	0	1	7
Sc	<1	9	<1	2	3	2	4	3	4	11	9	5	4	9
TOT/C	0.02	0.06	0.02	0.05	<0.02	0.06	0.03	<0.02	0.09	0.02	0.06	0.02	<0.02	0.06
TOT/S	<0.02	0.05	<0.02	<0.02	<0.02	<0.02	<0.02	<0.02	0.04	0.05	0.15	<0.02	<0.02	0.10
Eu/Eu*	0.57	0.61	0.55	0.60	0.51	0.72	0.56	0.60	0.45	0.78	0.73	0.74	0.60	0.73

Eu/Eu* ($Eu_N/[Sm_N+Gd_N]$) ratios were calculated using chondrite normalising values from Sun and McDonough (1989).
Note that samples DA14-304 and DA14-372 are duplicates of samples DA13-004 and DA13-072 respectively.

contradictory "arc-like" geochemical signatures could be inherited from the Antsiribe Nord and Manambato (Thomas et al., 2009), Imorona-Itsindro (Archibald et al., 2017), Dabolava (Archibald et al., 2018) and Betsiboka (Tucker et al., 1999; BGS-USGS-GLW, 2008) plutonic suites.

6.3. Zircon O and Hf isotopes

Zircon in equilibrium with mantle-derived melts have a restricted range of $\delta^{18}O$ concentrations (5.3‰ ± 0.6‰; Valley et al., 1998). Zircon $\delta^{18}O$ values above 5.3‰ ± 0.6‰ are recorded in rocks derived from melting or assimilation of supracrustal material that experienced low temperature water–rock interactions in a hydrological cycle at or near the surface (Valley et al., 2005). In contrast, $\delta^{18}O$ values less than 5.3‰ ± 0.6‰ signify high-T interactions of meteoric water with evolving magmas in shallow, sub-volcanic magma chambers (Bindeman, 2008). Ambalavao and Maevarano Suite samples from the Antananarivo Domain exhibit a wide range in zircon $^{18}O/^{16}O$ ratios (5.6 ± 0.7 to 7.3 ± 0.8), reflecting the diverse crustal sources found within the Precambrian basement. An alternative explanation is mixing between mantle-derived melts and high-$\delta^{18}O$ supracrustal melts or the assimilation of high-$\delta^{18}O$ crustal material into mantle-derived melts. Melting and/or assimilation of Antananarivo Domain rocks (see section 2.1) could result in a range of $\delta^{18}O$ values regardless of possible mantle input. A wide range of $\delta^{18}O$ values for the Imorona-Itsindro Suite in the Antananarivo and Manampotsy Domains (9.8‰ ± 0.3‰ to 4.2‰ ± 0.6‰) was interpreted to represent mixing of these crustal sources with a

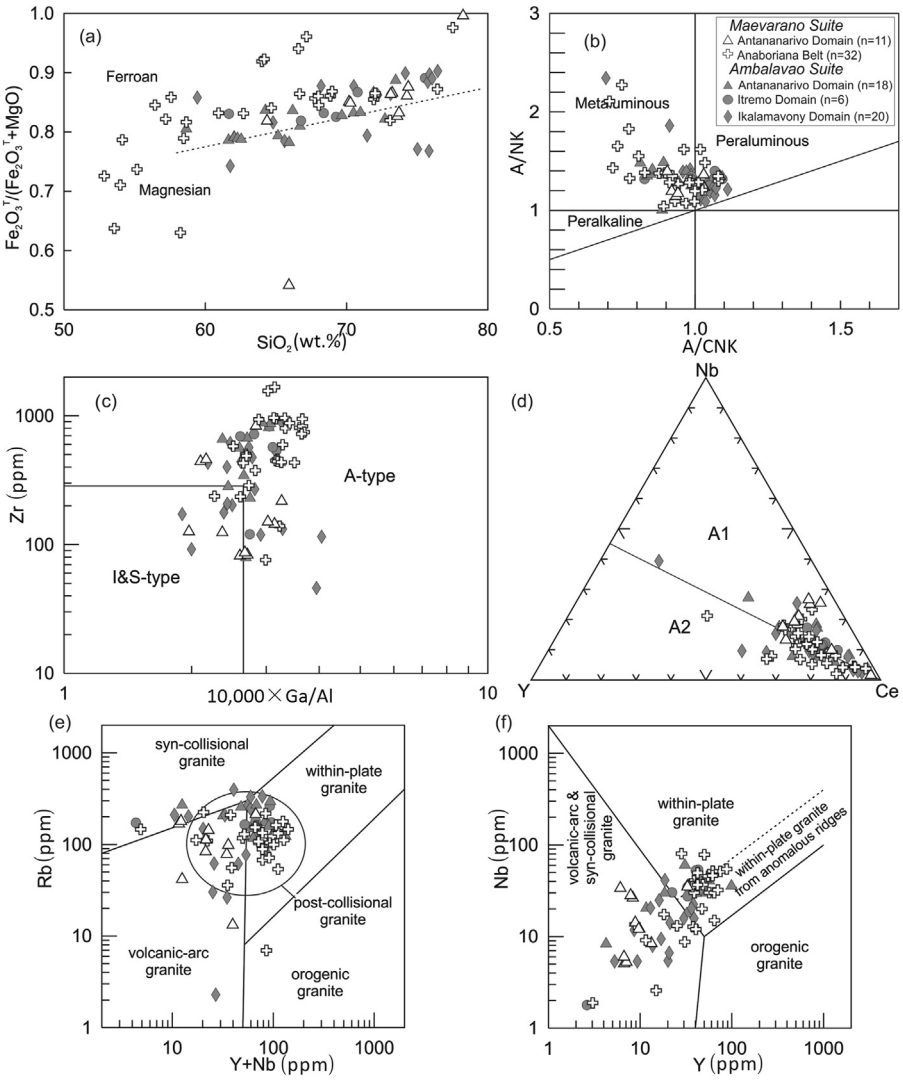

Figure 11. Classification diagrams for samples of the Ambalavao-Maevarano Suite: (a) Plot of SiO_2 versus $Fe_2O_3^T/(Fe_2O_3^T+MgO)$ with the ferroan–magnesian dividing line from Frost et al. (2001); (b) shand index plot. A/NK = molar $Al_2O_3/(Na_2O + K_2O)$; A/CNK = molar $Al_2O_3/(CaO + Na_2O + K_2O)$; (c) 10,000×Ga/Al versus Zr after Whalen et al. (1987) showing the I, S and A-type granite fields; (d) representation triangular plots for distinguishing A1 and A2 type granitoids. The dividing line for A1 versus A2 granitoids is Y/Nb = 1.2 (Eby, 1992); (e–f) tectonic discrimination plots for felsic rocks from Pearce et al. (1984). Post-collisional granite field in (e) is from Pearce (1996). Data are from Table 4 and the references listed in Fig. 4.

mantle component in a supra-subduction zone tectonic environment (Archibald et al., 2016).

$\varepsilon_{Hf}(t)$ values for these same Ediacaran samples from the Antananarivo Domain are mostly between −27.8 ± 2.6 and −12.3 ± 1.3. This array approximates the range expected for the ca. 3.0 Ga and 2.5 Ga Antananarivo Domain crust between ca. 600 Ma and 500 Ma (Fig. 12b). Zircon ε_{Hf}(2500 Ma) data for the Betsiboka Suite are between +0.7 and +3.8 (D.B. Archibald, unpublished data), and show only a minor deflection from the depleted-mantle curve at ca. 2500 Ma. The two Ediacaran samples that plot outside of the age corrected Antananarivo Domain evolution field (DA13-037 and DA13-041 on Fig. 12b), are more enriched in ^{176}Hf and are likely a consequence of increased mantle input or melting of a protolith with a more mantle-like isotopic signature. $\varepsilon_{Hf}(t)$ data for Cambrian granite in the Ambatondrazaka Region (Fig. 2) of the Antananarivo Domain are between −16.4 and −12.9 (Zhou et al., 2015). These values lie within the range expected for mixing of the Antananarivo Domain basement crustal melts with input from a mantle component (Fig. 14b). Nd isotopic data the Ambatondrazaka Granite (Zhou et al., 2015) show negative $\varepsilon_{Nd}(t)$ values (−24 and −23), indicating an ancient continental crustal source. Low initial $^{87}Sr/^{86}Sr$ ratios (0.7067 and 0.7069) were interpreted to indicate derivation from mafic crustal material with low Rb/Sr ratios (Zhou et al., 2015).

The isotopic characteristics of the rocks intruding the Itremo Group are consistent with metasedimentary rocks being incorporated into the evolving Ediacaran–Cambrian magmas (Fig. 14). Samples DA13-050 and DA13-051 were collected near the eastern edge of the Itremo Domain along the Betsileo Shear Zone (Fig. 2). $\delta^{18}O$ values are above the mantle derived zircon field. $\delta^{18}O$ values collected for the Imorona-Itsindro Suite in the Itremo Domain have lower $\delta^{18}O$ values between 4.6‰ and 5.4‰ (Archibald et al., 2016). Mantle, to slightly below mantle, $\delta^{18}O$ values were interpreted to indicate shallow intrusion and high-T meteoric water interaction as Tonian-aged rocks were emplaced in a continental arc (Archibald et al., 2016). Ediacaran samples in the Itremo Domain have $\varepsilon_{Hf}(t)$ values between −12.9 ± 2.2 and −20.5 ± 3.0 (Fig. 12b). These two samples and the two samples from the Antananarivo Domain with

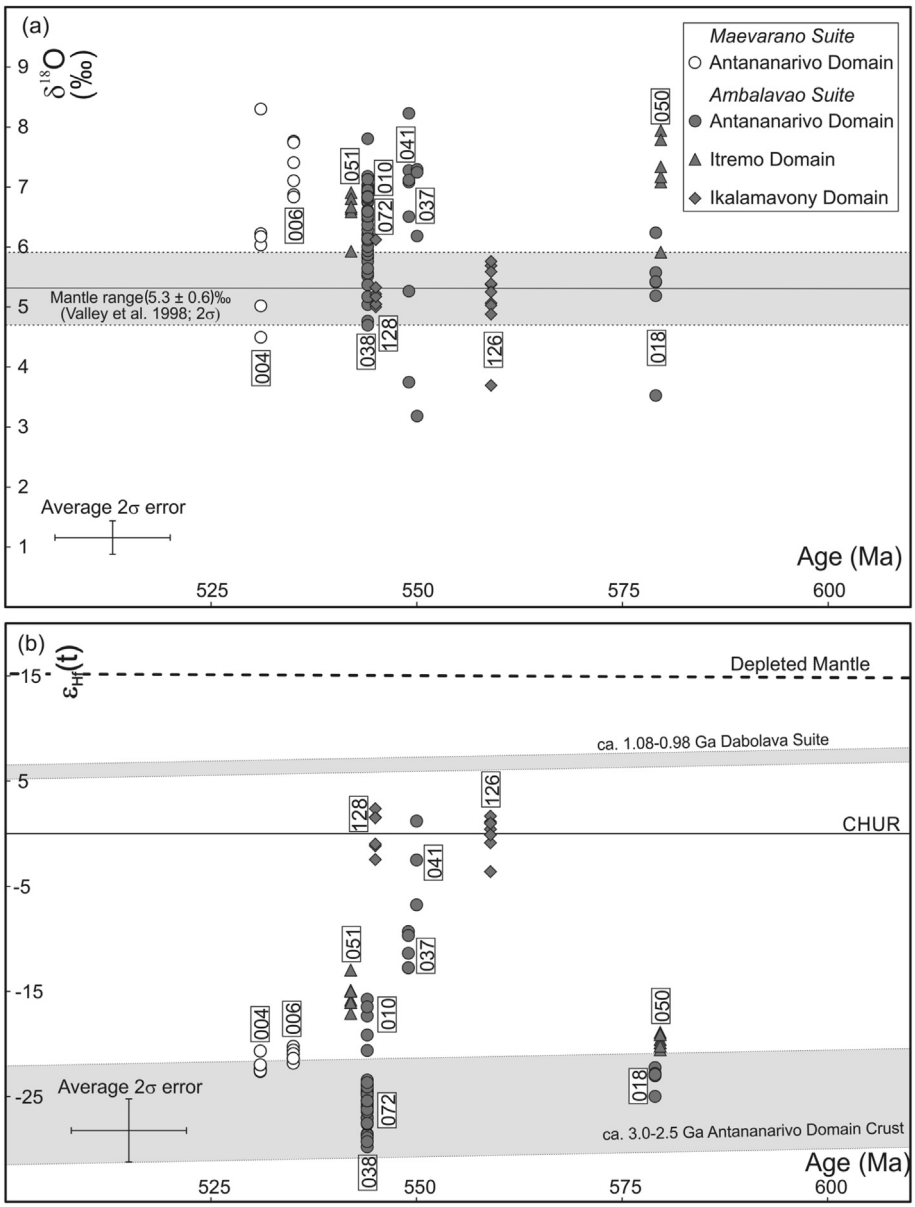

Figure 12. Oxygen and hafnium isotope diagrams for samples of the Ambalavao and Maevarano Suites. (a) $\delta^{18}O$ and (b) $\varepsilon_{Hf}(t)$ plotted against the interpreted sample crystallisation age. The range of mantle derived $\delta^{18}O$ (zircon) values is 5.3‰ ± 0.6‰ (Valley et al., 1998). The $T_{DM}{}^{C}$ Hf evolution fields are based on a $^{176}Lu/^{177}Hf$ ratio of 0.015 (Griffin et al., 2004). Abbreviations: DM = depleted mantle. CHUR = chondrite uniform reservoir. Note that the DA13-or DA14-prefixes are excluded from each sample number to improve diagram clarity.

the highest $\varepsilon_{Hf}(t)$ values are from locations near the Betsileo Shear Zone (Collins et al., 2000, 2003c). This shear zone forms the boundary between the Itremo and Antananarivo Domains that facilitated the ascent mantle melts and promoted the incorporation of crustal material.

Two samples (DA14-126 and DA14-128) from the Ikalamavony Domain have $\delta^{18}O$ values that plot within the mantle range (Fig. 12a) demonstrating that zircon crystallised from a mantle melt that experienced only minor crustal contamination or that zircon were derived by melting of a juvenile crustal material. $\delta^{18}O$ values for the Imorona-Itsindro Suite in the Ikalamavony Domain have a similar range (5.2‰–7.8‰) and were interpreted to be a result of incorporation of isotopically juvenile Ikalamavony Group and Dabolava Suite crust (Archibald et al., 2016). Ediacaran-aged samples have mean $\varepsilon_{Hf}(t)$ values near CHUR (0.0 ± 3.3 and 0.2 ± 4.6; Fig. 12b). $\varepsilon_{Hf}(t)$ data for the Mesoproterozoic Dabolava Suite (+7.5 to +16) indicates a mantle source with only minor involvement of primitive crust that was recycled within the arc (Archibald et al., 2018). $\varepsilon_{Hf}(t)$ data for zircon from the Imorona-Itsindro Suite (−4 to +14) are also relatively depleted in ^{176}Hf and were interpreted to result from crustal assimilation of primitive Dabolava Suite/Ikalamavony Group crust (Archibald et al., 2016). Therefore, melting or assimilation of Ikalamavony Domain rocks during the Ediacaran resulted in the more mantle-like Hf isotopic signatures recorded in Ambalavao Suite samples.

Imorona-Itsindro Suite $\delta^{18}O$ (2.8‰–10.2‰) and hafnium isotope data recalculated at 550 Ma (−30 to +2) show similar values to the Ambalavao and Maevarano Suites (Fig. 14). The Tonian-aged magmatic suite has geochemical signatures typical of arc-environments such as negative Nb-Ta, Sr-P and Ti anomalies and enrichment in LREEs and LILEs (Boger et al., 2014, 2015; Archibald et al., 2017). The Dabolava Suite also has arc-like geochemical characteristics but has more

primitive isotopic characteristics ($\delta^{18}O = 4.1‰–8.2‰$; ε_{Hf}(550 Ma): −3 to +5; Archibald et al., 2018). The Neoarchaean Betsiboka Suite has $\delta^{18}O$ values (3.8‰–8.0‰), recalculated ε_{Hf}(550 Ma) values (−39 to −50) and geochemical characteristics (BGS-USGS-GLW, 2008) that are compatible with an arc tectonic setting. Incorporation of any of these older arc plutonic rocks accounts for the contradictory arc-like geochemical signatures recorded in Ediacaran–Cambrian anorogenic plutonic rocks in Madagascar.

This study is the first documentation of oxygen and hafnium isotopic characteristics in zircon from Ediacaran–Cambrian detrital zircon sources in Madagascar, which are important for tracing source to sink pathways in Phanerozoic sedimentary rock provenance studies (e.g. Lloyd et al., 2016; Veevers, 2017). Ediacaran–Cambrian zircon from Madagascar exhibit isotopically evolved compositions compared to rocks emplaced concurrently elsewhere in the EAO. For example, in the Western ANS, Hf isotopic compositions of Ediacaran zircon ($\varepsilon_{Hf}(t)$ values between +5 and + 10; Robinson et al., 2014) are more juvenile than Hf isotopic contents recorded by Ediacaran zircon in Madagascar. Ediacaran granite in Ethiopia yielded $\varepsilon_{Hf}(t)$ values between +6.7 and + 7.9 (Blades et al., 2015). Ediacaran–Cambrian (ca. 575–506 Ma) mainly granitic rocks in the Sør Rondane Mountains have zircon $\varepsilon_{Hf}(t)$ values between +6.2 and −8.3 (Elburg et al., 2016). The zircon Hf compositions from the Ambalavao and Maevarano Suites represent a distinct detrital zircon source region for isotopically evolved Ediacaran–Cambrian zircon Hf isotopic signatures ($\varepsilon_{Hf}(t)$ as low as −28) for Phanerozoic sedimentary provenance studies (e.g., Squire et al., 2006).

6.4. Tectonic implications

Goodenough et al. (2010) noted that significant crustal involvement was unlikely given the absence of xenocrystic zircon in Maevarano Suite rocks. In light of our new zircon oxygen and hafnium isotopic data, however, crustal materials appear to have played a vital role in magma genesis. Many Ediacaran–Cambrian zircon grains, especially those from the Antananarivo and Itremo Domains have crustal Hf isotopic signatures (Fig. 12b). Enclaves and xenoliths are common in Ambalavao Suite rocks (BGS-USGS-GLW, 2008) indicating crustal assimilation processes. Crustal anatexis was also feasible given that peak high-T (>800 °C) metamorphism at ca. 550 Ma (Markl et al., 2000; Buchwaldt et al., 2003; CGS, 2009) in Madagascar was above the melting point of hydrated crust (Thompson and Connolly, 1995; Holtz et al., 2001).

Intense transcurrent tectonics, active deformation and high heat flow facilitated and promoted crustal contamination of evolving magmas that intruded along active shear zones. Because the ascending mafic magmas incorporated crustal material, it is unlikely that samples retained their original mantle isotopic signature if mantle melts were, in fact, significantly involved in magma genesis. Rather, these rocks represent crustal probes and reflect the isotopic composition of the deep crust of central Madagascar. These isotopic signatures broadly reflect the components of the lithotectonic domain (i.e. Antananarivo, Itremo or Ikalamavony Domain) that the sample intruded (Fig. 1b). Ediacaran–Cambrian zircon from the Antananarivo and Itremo Domains have crustal Hf isotopic signals whereas Ediacaran zircon from the Ikalamavony Domain have more mantle-like Hf isotopic compositions.

Isotopic and geochemical data presented here support the magma emplacement mechanisms proposed for the Maevarano Suite by Goodenough et al. (2010), in which the plutonic rocks were emplaced in a late syn- to post-collisional tectonic setting following the model of Bonin (2004). Regions that experienced older subduction events are often underlain by hydrated and metasomatised subcontinental lithospheric mantle (SCLM), thickened by mafic intrusion and underplating. Thickening, cooling and garnet growth all contribute to densification and ultimately to delamination, partial melting and asthenospheric influx (Bonin, 2004; Elkins-Tanton, 2005). This delamination leads to thinning of the

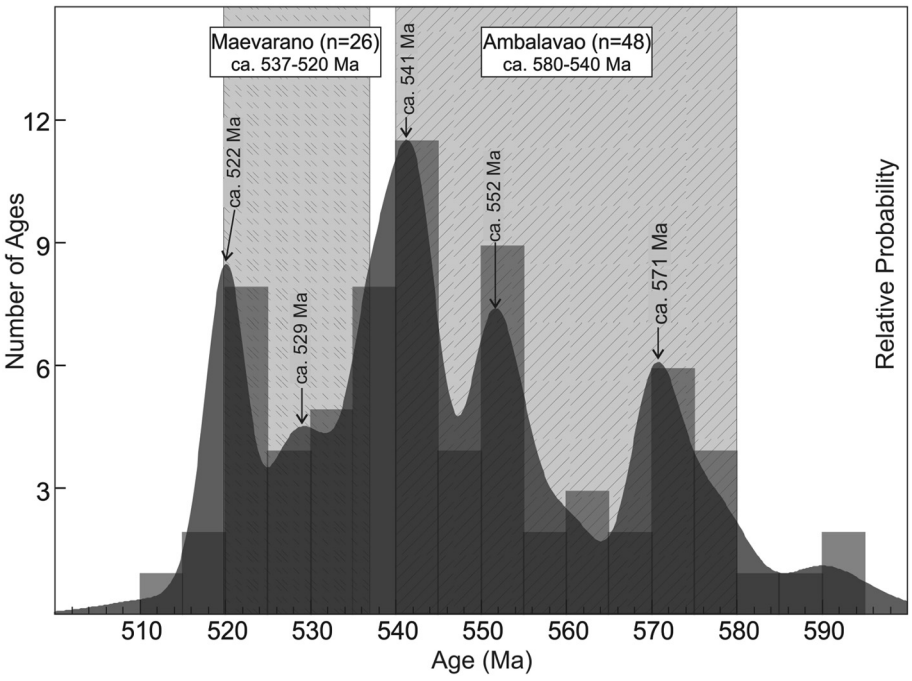

Figure 13. Kernel density plot and histogram for all available geochronological data for late Ediacaran–Cambrian magmatism in Madagascar. Included in this are data from this study, Paquette et al. (1994), Paquette and Nédélec (1998), Kröner et al. (1999, 2000), Müller (2000), de Wit et al. (2001), Meert et al. (2001b), Buchwaldt et al. (2003), Tucker et al. (2007), BGS-USGS-GLW (2008), GAF-BGR (2008a,b,c), CGS (2009), Goodenough et al. (2010), JICA (2012) and Zhou et al. (2015). Data were plotted using Density Plotter (Vermeesch, 2012) and histogram bin sizes are 5 Ma. Magma emplacement intervals for each suite are from this study, BGS-USGS-GLW (2008) and Goodenough et al. (2010).

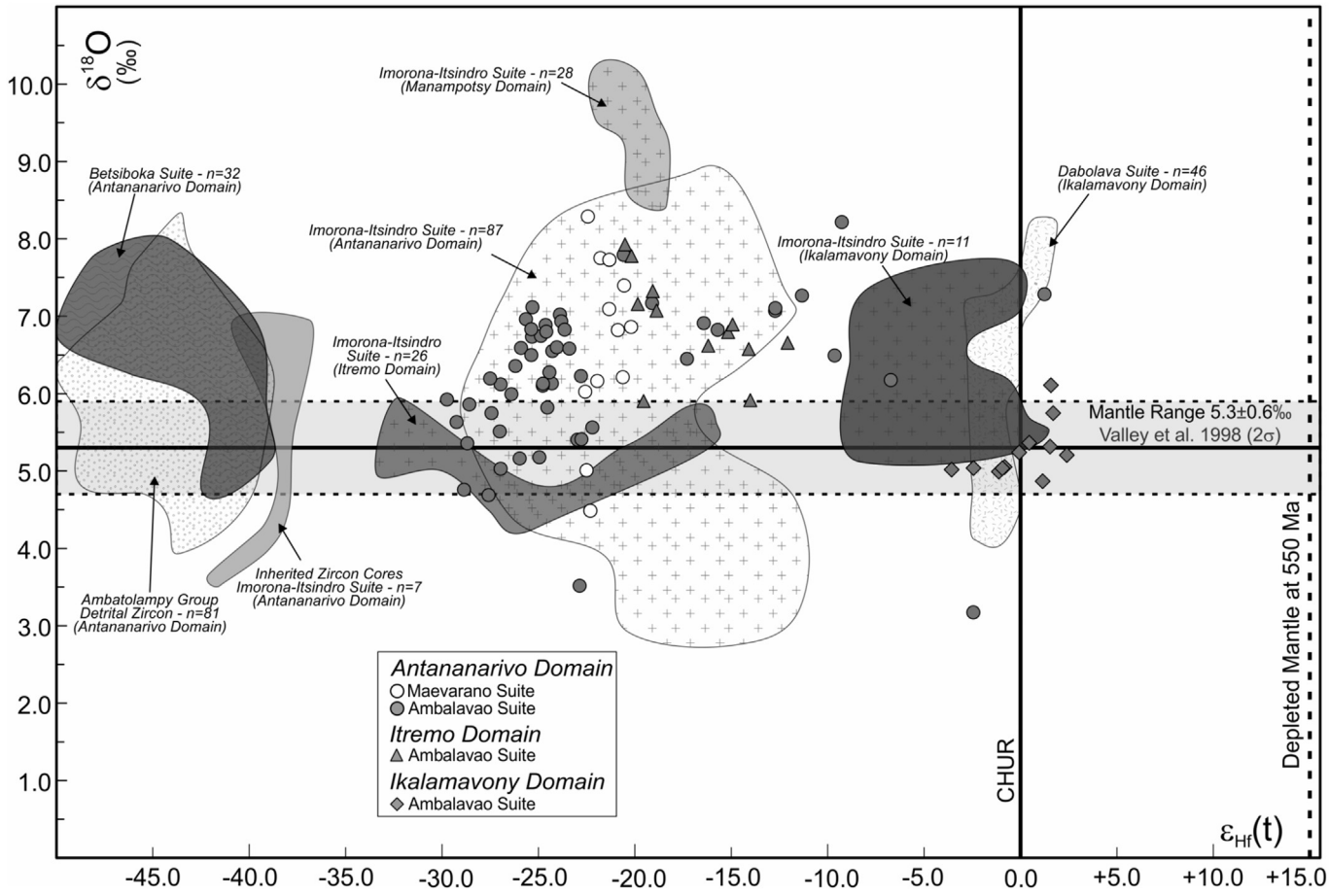

Figure 14. $\varepsilon_{Hf}(t)$ plotted against $\delta^{18}O$ for samples of the Ambalavao and Maevarano Suites. Data for the Ambatolampy Group detrital zircon that were interpreted to be derived from the Antananarivo Domain basement are from Archibald et al. (2015). Imorona-Itsindro Suite and inherited zircon core data are from Archibald et al. (2016). Betsiboka Suite data are from four Neoarchaean–Palaeoproterozoic granite orthogneiss samples (D.B. Archibald, unpublished). Data for the Dabolava Suite are from (Archibald et al., 2018). The fields on the diagram were calculated using Hf data age corrected to 550 Ma using the methods of Griffin et al. (2002) with a $^{176}Lu/^{177}Hf$ decay constant of 0.015. The numbers of zircon used to construct each field are listed alongside the appropriate field. At most, three zircon were considered outliers (Imorona-Itsindro Suite in the Antananarivo Domain), and omitted. The remaining fields include all data or omit only one outlier analysis. The range of mantle-derived $\delta^{18}O$ composition is from Valley et al. (1998).

lithosphere and heating the crust by hot asthenospheric mantle and by the derived mafic melts (Elkins-Tanton, 2005). Accordingly, like Goodenough et al. (2010), the Ambalavao and Maevarano Suites are interpreted to be a result of a post-collisional stage where delamination removed part of the lithospheric mantle and induced melting in the upper SCLM. This model suggests a mafic magmatic flux to the crust, partly derived from the SCLM that was previously metasomatised during the pre-Ediacaran subduction events and partly from new asthenospheric upwelling. This phase of lithospheric delamination occurred in the early Cambrian following the final collision of Neoproterozoic India with the previously amalgamated Africa/Azania continents (Collins and Pisarevsky, 2005; Merdith et al., 2017).

7. Summary and conclusions

The Ambalavao and Maevarano Suites represent mainly granitoid magmatism emplaced in the Ediacaran–Cambrian during the waning stages of the amalgamation of Gondwana. Geochronological data illustrates essentially continuous magmatism from the Ediacaran into the Cambrian with the emplacement of the Ambalavao (ca. 580–540 Ma) and Maevarano (ca. 537–522 Ma) Suites. The plutonic suites correspond temporally and spatially with late-Neoproterozoic shear zones and are intimately associated with intense regional deformation and metamorphism. Whole-rock geochemical data for both suites are indistinguishable and characterised by coherent fractionation trends of major elements, enrichment of HFSEs, LILEs, and REEs (especially the LREEs). These geochemical features are compatible with magma genesis in an anorogenic (A-type) late syn- to post-collisional tectonic setting. Magmatic zircon oxygen and hafnium isotopic data indicate a significant crustal component during magma genesis. Zircon shows little evidence for inheritance of ancient U-Pb ages implying high-temperature magmatism and assimilation above the zircon saturation temperature, but zircon O and Hf isotopic data indicate both suites incorporated crustal material by crustal anatexis or assimilation. The zircon $\varepsilon_{Hf}(t)$ data show slightly positive but mostly negative values, suggesting involvement of both juvenile mantle material and reworked ancient crustal components. Isotopic data also mimic the different basement components of central Madagascar, in particular, the juvenile nature of the Mesoproterozoic Ikalamavony Domain relative to the Antananarivo and Itremo Domains. Therefore, the isotopic features of Ediacaran–Cambrian intrusive rocks could be used as a tool to map distinct and/or linked terranes in Madagascar or other terranes using the isotopic characteristics of intrusive rocks. The evolved Hf isotopic character of Ediacaran–Cambrian zircon from Madagascar is unlike more juvenile Ediacaran–Cambrian zircon found elsewhere in the EAO and may provide a distinct detrital zircon source region for Phanerozoic sedimentary rock provenance studies.

Acknowledgements

Ms. Aoife McFadden and Dr. Benjamin Wade (Adelaide Microscopy) are acknowledged for assistance obtaining CL images and LA-ICP-MS U-Pb data. K. Goodenough and R. Schmitt provided insightful comments that significantly improved the quality of this manuscript. A. Nédélec, B. Bingen and an anonymous reviewer provided constructive criticism on an earlier version of this manuscript. This paper forms TRaX record 410 and is an output of ARC Future Fellowship grant FT120100340. This paper is a contribution to IGCP projects #628 (Gondwana Map) and #648 (Supercontinent Cycles and Global Geodynamics).

Appendix A. Supplementary data

Supplementary data to this article can be found online at https://doi.org/10.1016/j.gsf.2018.07.007.

References

Archibald, D.B., Collins, A.S., Foden, J.D., Payne, J.L., Holden, P., Razakamanana, T., De Waele, B., Thomas, R.J., Pitfield, P.E.J., 2016. Genesis of the Tonian Imorona-Itsindro magmatic suite in central Madagascar: insights from U-Pb, oxygen and hafnium isotopes in zircon. Precambrian Research 281, 312–337.

Archibald, D.B., Collins, A.S., Foden, J.D., Payne, J.L., Macey, P.H., Holden, P., Razakamanana, T., 2018. Stenian–tonian arc magmatism in west central Madagascar: the genesis of the Dabolava suite. Journal of the Geological Society 175, 111–129.

Archibald, D.B., Collins, A.S., Foden, J.D., Payne, J.L., Taylor, R., Holden, P., Razakamanana, T., Clark, C., 2015. Towards unravelling the Mozambique Ocean conundrum using a triumvirate of zircon isotopic proxies on the Ambatolampy Group, central Madagascar. Tectonophysics 662, 167–182.

Archibald, D.B., Collins, A.S., Foden, J.D., Razakamanana, T., 2017. Tonian arc magmatism in Central Madagascar: the petrogenesis of the Imorona-Itsindro suite. The Journal of Geology 125 (3), 271–297.

Armistead, S.E., Collins, A.S., Payne, J.L., Foden, J.D., De Waele, B., Shaji, E., Santosh, M., 2018. A re-evaluation of the Kumta Suture in western peninsular India and its extension into Madagascar. Journal of Asian Earth Sciences 157, 317–328.

Bauer, W., Walsh, G.J., de Waele, B., Thomas, R.J., Horstwood, M.S.A., Bracciali, L., Schofield, D.I., Wollenberg, U., Lidke, D.J., Rasaona, I.T., Rabarimanana, M.H., 2011. Cover sequences at the northern margin of the Antongil Craton, NE Madagascar. Precambrian Research 189 (3–4), 292–312.

Be'eri-Shlevin, Y., Katzir, Y., Whitehouse, M., 2009. Post-collisional tectono-magmatic evolution in the northern Arabian–Nubian Shield: time constraints from ion-probe U-Pb dating of zircon. Journal of the Geological Society 166 (1), 71–85.

BGS-USGS-GLW, 2008. Revision de la cartographie geologique et miniere des zones Nord, Centre, et Centre Est de Madagascar. BGS Report CR/08/078. Keyworth, England.

Bindeman, I.N., 2008. Oxygen isotopes in mantle and crustal magmas as revealed by single crystal analysis in Minerals, Inclusions and Volcanic Processes ed. Putirka, K.D. and Tepley III, F.J. Reviews in Mineralogy and Geochemistry vol. 69, 445–478.

Bingen, B., Jacobs, J., Viola, G., Henderson, I.H.C., Skår, Ø., Boyd, R., Thomas, R.J., Solli, A., Key, R.M., Daudi, E.X.F., 2009. Geochronology of the Precambrian crust in the Mozambique belt in NE Mozambique, and implications for Gondwana assembly. Precambrian Research 170 (3–4), 231–255.

Blades, M.L., Collins, A.S., Foden, J., Payne, J.L., Xu, X., Alemu, T., Woldetinsae, G., Clark, C., Taylor, R.J.M., 2015. Age and hafnium isotopic evolution of the Didesa and Kemashi Domains, western Ethiopia. Precambrian Research 270, 267–284.

Blades, M.L., Foden, J., Collins, A.S., Alemu, T., Woldetinsae, G., 2017. The origin of the ultramafic rocks of the Tulu Dimtu Belt, western Ethiopia – do they represent remnants of the Mozambique Ocean? Geological Magazine 1–21.

Boger, S.D., Hirdes, W., Ferreira, C.A.M., Schulte, B., Jenett, T., Fanning, C.M., 2014. From passive margin to volcano–sedimentary forearc: the Tonian to Cryogenian evolution of the Anosyen Domain of southeastern Madagascar. Precambrian Research 247, 159–186.

Boger, S.D., Hirdes, W., Ferreira, C.A.M., Schulte, B., Jenett, T., Fanning, C.M., 2015. Reply to comment by J-L Zhou on "From passive margin to volcano-sedimentary forearc: the Tonian to Cryogenian evolution of the Anosyen Domain of southeastern Madagascar" by Boger et al. Precambrian Research, Volume 247, July 2014, Pages 159–186. Precambrian Research 262, 127–130.

Bonin, B., 2004. Do coeval mafic and felsic magmas in post-collisional to within-plate regimes necessarily imply two contrasting, mantle and crustal, sources? A review. Lithos 78 (1), 1–24.

Buchwaldt, R., Tucker, R.D., Dymek, R.F., 2003. Geothermobarometry and U-Pb Geochronology of metapelitic granulites and pelitic migmatites from the Lokoho region, Northern Madagascar. American Mineralogist 88, 1753–1768.

CGS, 2009. Map Explanation of 1:100 000 scale (Zone E) Sheets I46 – Ambararata, J46 – Beopoaka, 47 – Itondy, J47 – Belobaka, K47 – Ambatofotsy, I48 – Miandrivazo, J48 – Betrondro, K48 – Ambatondradama, I49 – Ankotrofotsy, J49 – Dabolava, K49 – Anjoma-Ramartina, L49 – Vasiana, M49 – Ankazomiriotra, N49 – Antsirabe. , République de Madagascar, Ministère de L'Energie et des Mines – Project de Gouvernance des Ressources Minérales, Antananarivo, Madagascar and Council for Géoscience, Pretoria, South Africa (in French).

Collins, A.S., 2006. Madagascar and the amalgamation of central Gondwana. Gondwana Research (GR Focus) 9, 3–16.

Collins, A.S., Fitzsimons, I.C.W., Hulscher, B., Razakamanana, T., 2003a. Structure of the eastern margin of the east African orogen in central Madagascar. Precambrian Research 123, 111–133.

Collins, A.S., Johnson, S., Fitzsimons, I.C.W., Powell, C.M., Hulscher, B., Abello, J., Razakamanana, T., 2003b. Neoproterozoic deformation in central Madagascar: a structural section through part of the East African Orogen. In: Yoshida, M., Windley, B., Dasgupta, S. (Eds.), Proterozoic East Gondwana: Supercontinent Assembly and Breakup, vol. 206. Special Publication of the Geological Society, London, pp. 363–379.

Collins, A.S., Kröner, A., Fitzsimons, I.C.W., Razakamanana, T., 2003c. Detrital footprint of the Mozambique ocean: U/Pb SHRIMP and Pb evaporation zircon geochronology of metasedimentary gneisses in eastern Madagascar. Tectonophysics 375, 77–99.

Collins, A.S., Pisarevsky, S.A., 2005. Amalgamating eastern Gondwana: the evolution of the Circum-Indian orogens. Earth Science Reviews 71, 229–270.

Collins, A.S., Razakamanana, T., Windley, B.F., 2000. Neoproterozoic extensional detachment in central Madagascar: implications for the collapse of the East African Orogen. Geological Magazine 137, 39–51.

Collins, A.S., Windley, B.F., 2002. The tectonic evolution of central and northern Madagascar and its place in the final assembly of Gondwana. The Journal of Geology 110, 325–340.

Cox, G.M., Lewis, C.J., Collins, A.S., Halverson, G.P., Jourdan, F., Foden, J., Nettle, D., Kattan, F., 2012. Ediacaran terrane accretion within the Arabian–Nubian shield. Gondwana Research 21 (2–3), 341–352.

Cox, R., Coleman, D.S., Chokel, C.B., DeOreo, S.B., Collins, A.S., Kröner, A., De Waele, B., 2004. Proterozoic tectonostratigraphy and paleogeography of central Madagascar derived from detrital zircon U-Pb age populations. The Journal of Geology 112, 379–400.

da Silva Schmitt, R., de Araújo Fragoso, R., Collins, A.S., 2018. Suturing Gondwana in the Cambrian: the Orogenic Events of the Final Amalgamation, Geology of Southwest Gondwana. Springer, pp. 411–432.

De Waele, B., Thomas, R.J., Macey, P.H., Horstwood, M.S.A., Tucker, R.D., Pitfield, P.E.J., Schofield, D.I., Goodenough, K.M., Bauer, W., Key, R.M., Potter, C.J., Armstrong, R.A., Miller, J.A., Randriamananjara, T., Ralison, V., Rafahatelo, J.M., Rabarimanana, M., Bejoma, M., 2011. Provenance and tectonic significance of the Palaeoproterozoic metasedimentary successions of central and northern Madagascar. Precambrian Research 189 (1–2), 18–42.

de Wit, M.J., Bowring, S.A., Ashwal, L.D., Randrianasolo, L.G., Morel, V.P.I., Rambeloson, R.A., 2001. Age and Tectonic Evolution of Neoproterozoic ductile shear zones in southwestern Madagascar, with implications for Gondwana studies. Tectonics 20, 1–45.

Eby, G.N., 1992. Chemical subdivision of the A-type granitoids:Petrogenetic and tectonic implications. Geology 20 (7), 641–644.

Elburg, M.A., Andersen, T., Jacobs, J., Läufer, A., Ruppel, A., Krohne, N., Damaske, D., 2016. One hundred fifty million years of intrusive activity in the Sør Rondane Mountains (east Antarctica): implications for Gondwana assembly. The Journal of Geology 124 (1), 1–26.

Elkins-Tanton, L.T., 2005. Continental magmatism caused by lithospheric delamination. Geological Society of America Special Papers 388, 449–461.

Fitzsimons, I.C.W., 2003. Proterozoic basement provinces of southern and south-western Australia, and their correlation with Antarctica. Geological Society, London, Special Publications 206 (1), 93–130.

Fritz, H., Abdelsalam, M., Ali, K.A., Bingen, B., Collins, A.S., Fowler, A.R., Ghebreab, W., Hauzenberger, C.A., Johnson, P.R., Kusky, T.M., Macey, P., Muhongo, S., Stern, R.J., Viola, G., 2013. Orogen styles in the east African orogen: a review of the Neoproterozoic to Cambrian tectonic evolution. Journal of African Earth Sciences 86 (0), 65–106.

Frost, B.R., Barnes, C.G., Collins, W.J., Arculus, R.J., Ellis, D.J., Frost, C.D., 2001. A geochemical classification for granitic rocks. Journal of Petrology 42 (11), 2033–2048.

Frost, C.D., Frost, B.R., 2010. On ferroan (A-type) granitoids: their compositional variability and modes of origin. Journal of Petrology 52 (1), 39–53.

GAF-BGR, 2008a. Final Report. Explanatory notes for the Androyan domain southern Madagascar. Réalisation des travaux de cartographie géologique de Madagascar, révision approfondie de la cartographie géologique et minière aux échelles 1/100,000 et 1/500,000 zone Sud. République de Madagascar, Ministère de l'Energie et des Mines (MEM/SG/DG/UCP/PGRM). 81 (in French).

GAF-BGR, 2008b. Final Report. Explanatory notes for the Anosyan domain southeast Madagascar. Réalisation des travaux de cartographie géologique de Madagascar, révision approfondie de la cartographie géologique et minière aux échelles 1/100,000 et 1/500,000 zone Sud. République de Madagascar, Ministère de l'Energie et des Mines (MEM/SG/DG/UCP/PGRM) (in French).

GAF-BGR, 2008c. Final Report. Explanatory notes for the Vohibory domain southwest Madagascar. Réalisation des travaux de cartographie géologique de Madagascar, révision approfondie de la cartographie géologique et minière aux échelles 1/100,000 et 1/500,000 zone Sud. République de Madagascar, Ministère de l'Energie et des Mines (MEM/SG/DG/UCP/PGRM) (in French).

GAF-BGR, 2008d. Final Report: Explanatory notes for the Ikalamavony domain, central and western Madagascar. Réalisation des travaux de cartographie géologique de Madagascar, révision approfondie de la cartographie géologique et minière aux échelles 1/100 000 et 1/500 000 zone Sud. République de Madagascar, Ministère de l'Energie et des Mines MEM/SG/DG/UCP/PGRM) (in French).

Goodenough, K.M., Thomas, R.J., De Waele, B., Key, R.M., Schofield, D.I., Bauer, W., Tucker, R.D., Rafahatelo, J.M., Rabarimanana, M., Ralison, A.V., Randriamananjara, T., 2010. Post-collisional magmatism in the central East African orogen: the Maevarano suite of north Madagascar. Lithos 116 (1–2), 18–34.

Grégoire, V., Nédélec, A., Monié, P., Montel, J.-M., Ganne, J., Ralison, B., 2009. Structural reworking and heat transfer related to the late-Panafrican Angavo shear zone of Madagascar. Tectonophysics 477 (3–4), 197–216.

Griffin, W.L., Belousova, E.A., Shee, S.R., Pearson, N.J., O'Reilly, S.Y., 2004. Archean crustal evolution in the northern Yilgarn Craton: U-Pb and Hf-isotope evidence from detrital zircons. Precambrian Research 131 (3–4), 231–282.

Griffin, W.L., Wang, X., Jackson, S.E., Pearson, N.J., O'Reilly, S.Y., Xu, X., Zhou, X., 2002. Zircon chemistry and magma mixing, SE China: in-situ analysis of Hf isotopes, Tonglu and Pingtan igneous complexes. Lithos 61 (3–4), 237–269.

Holtz, F., Becker, A., Wilhelm, J., 2001. The water-undersaturated and dry Qz-Ab-Or system revisited. Experimental results at very low water activities and geological implications. Contributions to Mineralogy and Petrology 141 (3), 347.

Ickert, R.B., Hiess, J., Williams, I.S., Holden, P., Ireland, T.R., Lanc, P., Schram, N., Foster, J.J., Clement, S.W., 2008. Determining high precision, in situ, oxygen isotope ratios with a SHRIMP II: analyses of MPI-DING silicate-glass reference materials and zircon from contrasting granites. Chemical Geology 257 (1–2), 114–128.

Jackson, S.E., Pearson, N.J., Griffin, W.L., Belousova, E.A., 2004. The application of laser ablation-inductively coupled plasma-mass spectrometry to in situ U-Pb zircon geochronology. Chemical Geology 211 (1–2), 47–69.

Jacobs, J., Bingen, B., Thomas, R.J., Bauer, W., Wingate, M.T.D., Feitio, P., 2008. Early Palaeozoic orogenic collapse and voluminous late-tectonic magmatism in Dronning Maud Land and Mozambique: insights into the partially delaminated orogenic root of the East African–Antarctic Orogen? Geological Society, London, Special Publications 308 (1), 69–90.

Jacobs, J., Elburg, M., Läufer, A., Kleinhanns, I.C., Henjes-Kunst, F., Estrada, S., Ruppel, A.S., Damaske, D., Montero, P., Bea, F., 2015. Two distinct late mesoproterozoic/early Neoproterozoic basement provinces in central/eastern Dronning Maud Land, east Antarctica: the missing link, 15–21° E. Precambrian Research 265, 249–272.

JICA, 2012. Results of SHRIMP dating in the Survey Area (Ishizaki, Shunichi), Final Report of U-Pb Geochronology, Project de Gouvernance des Ressources Minerales, Madagascar (PGRM) : Geological Mapping and Mineral Information System Project for the Ministère de l'Energie et des Mines (MEM/SG/DG/UCP/PGRM), Japanese International Cooperation Agency (in French).

Johnson, P.R., Andresen, A., Collins, A.S., Fowler, A.R., Fritz, H., Ghebreab, W., Kusky, T., Stern, R.J., 2011. Late Cryogenian–Ediacaran history of the Arabian–Nubian Shield: a review of depositional, plutonic, structural, and tectonic events in the closing stages of the northern East African Orogen. Journal of African Earth Sciences 61 (3), 167–232.

Jöns, N., Emmel, B., Schenk, V., Razakamanana, T., 2009. From orogenesis to passive margin—the cooling history of the Bemarivo Belt (N Madagascar), a multi-thermochronometer approach. Gondwana Research 16 (1), 72–81.

Key, R.M., Pitfield, P.E.J., Thomas, R.J., Goodenough, K.M., De Waele, B., Schofield, D.I., Bauer, W., Horstwood, M.S.A., Styles, M.T., Conrad, J., Encarnacion, J., Lidke, D.J., O'Connor, E.A., Potter, C., Smith, R.A., Walsh, G.J., Ralison, A.V., Randriamananjara, T., Rafahatelo, J.-M., Rabarimanana, M., 2011. Polyphase Neoproterozoic orogenesis within the east Africa–Antarctica orogenic belt in central and northern Madagascar. Geological Society, London, Special Publications 357 (1), 49–68.

Kröner, A., Hegner, E., Collins, A.S., Windley, B.F., Brewer, T.S., Razakamanana, T., Pidgeon, R.T., 2000. Age and magmatic history of the Antananarivo Block, central Madagascar, as derived from zircon geochronology and Nd isotopic systematics. American Journal of Science 300 (4), 251–288.

Kröner, A., Windley, B.F., Jaeckel, P., Brewer, T.S., Razakamanana, T., 1999. New zircon ages and regional significance for the evolution of the Pan-African orogen in Madagascar. Journal of the Geological Society, London 156, 1125–1135.

Küster, D., Harms, U., 1998. Post-collisional potassic granitoids from the southern and northwestern parts of the Late Neoproterozoic East African Orogen: a review. Lithos 45 (1–4), 177–195.

Lloyd, J., Collins, A.S., Payne, J.L., Glorie, S., Holford, S., Reid, A.J., 2016. Tracking the Cretaceous transcontinental Ceduna River through Australia: the hafnium isotope record of detrital zircons from offshore southern Australia. Geoscience Frontiers 7 (2), 237–244.

Markl, G., Bäuerle, J., Grujic, D., 2000. Metamorphic evolution of Pan-African granulite facies metapelites from Southern Madagascar. Precambrian Research 102 (1–2), 47–68.

Martelat, J.-E., Lardeaux, J.-M., Nicollet, C., Rakotondrazafy, R., 2000. Strain pattern and late Precambrian deformation history in southern Madagascar. Precambrian Research 102 (1–2), 1–20.

Martin, E.L., Collins, W.J., Kirkland, C.L., 2017. An Australian Source for Pacific-Gondwanan Zircons: Implications for the Assembly of Northeastern Gondwana. Geology 45 (8), 699–702.

Meert, J.G., 2003. A synopsis of events related to the assembly of eastern Gondwana. Tectonophysics 362, 1–40.

Meert, J.G., Hall, C., Nédélec, A., Razanatseheno, M.O.M., 2001a. Cooling of a late-syn orogenic pluton: evidence from laser K-feldspar modelling of the Carion granite, Madagascar. Gondwana Research 4 (3), 541–550.

Meert, J.G., Nédélec, A., Hall, C., Wingate, M.T.D., Rakotondrazafy, M., 2001b. Paleomagnetism, geochronology and tectonic implications of the Cambrian-age Carion granite, Central Madagascar. Tectonophysics 340 (1–2), 1–21.

Merdith, A.S., Collins, A.S., Williams, S.E., Pisarevsky, S., Foden, J.D., Archibald, D.B., Blades, M.L., Alessio, B.L., Armistead, S., Plavsa, D., Clark, C., Müller, R.D., 2017. A full-plate global reconstruction of the Neoproterozoic. Gondwana Research 50, 84–134.

Moine, B., Bosse, V., Paquette, J.-L., Ortega, E., 2014. The occurrence of a Tonian–Cryogenian (~850Ma) regional metamorphic event in Central Madagascar and the geodynamic setting of the Imorona–Itsindro (~800Ma) magmatic suite. Journal of African Earth Sciences 94 (0), 58–73.

Müller, B., 2000. The Evolution and Significance of the Bongolava–ranotsara Shear Zone, Madagascar. Rand Afrikaans University, Johannesburg, South Africa, p. 125.

Murphy, J.B., 2007. Igneous rock associations 8. Arc magmatism II: geochemical and isotopic characteristics. Geoscience Canada 34 (1), 7–35.

Nédélec, A., Paquette, J.-L., Antonio, P., Paris, G., Bouchez, J.-L., 2016. A-type stratoid granites of Madagascar revisited: age, source and links with the breakup of Rodinia. Precambrian Research 280, 231–248.

Nédélec, A., Ralison, B., Bouchez, J.-L., Grégoire, V., 2000. Structure and metamorphism of the granitic basement around Antananarivo: a key to the Pan-African history of central Madagascar and its Gondwana connections. Tectonics 19, 997–1020.

Paquette, J.-L., Nédélec, A., 1998. A new insight into Pan-African tectonics in the East–West Gondwana collision zone by U-Pb zircon dating of granites from central Madagascar. Earth and Planetary Science Letters 155 (1–2), 45–56.

Paquette, J.L., Nédélec, A., Moine, B., Rakotondrazafy, M., 1994. U-Pb, single zircon Pb-evaporation, and Sm–Nd isotopic study of a granulite domain in SE Madagascar. The Journal of Geology 102, 523–538.

Payne, J.L., Pearson, N.J., Grant, K.J., Halverson, G.P., 2013. Reassessment of relative oxide formation rates and molecular interferences on in situ lutetium-hafnium analysis with laser ablation MC-ICP-MS. Journal of Analytical Atomic Spectrometry 28 (7), 1068–1079.

Pearce, J.A., 1996. Sources and settings of granitic rocks. Episodes 19, 120–125.

Pearce, J.A., Harris, N.B.W., Tindle, A.G., 1984. Trace element discrimination diagrams for the tectonic interpretation of granitic rocks. Journal of Petrology 25 (4), 956–983.

Plavsa, D., Collins, A.S., Foden, J.D., Clark, C., 2015. The evolution of a Gondwanan collisional orogen: a structural and geochronological appraisal from the Southern Granulite Terrane, South India. Tectonics 34 (5), 820–857.

Raharimahefa, T., Kusky, T.M., 2010. Temporal evolution of the Angavo and related shear zones in Gondwana: constraints from LA-MC-ICP-MS U-Pb zircon ages of granitoids and gneiss from central Madagascar. Precambrian Research 182 (1–2), 30–42.

Raharimahefa, T., Kusky, T.M., Toraman, E., Rasoazanamparany, C., Rasaonina, I., 2013. Geometry and kinematics of the late proterozoic Angavo shear zone, Central Madagascar: implications for Gondwana assembly. Tectonophysics 592, 113–129.

Razanatseheno, M.O.M., Nédélec, A., Rakotondrazafy, M., Meert, J.G., Ralison, B., 2009. Four-stage building of the Cambrian Carion pluton (Madagascar). Earth and Environmental Science Transactions of the Royal Society of Edinburgh 100 (Special Issue 1–2), 133–145.

Robinson, F.A., Foden, J.D., Collins, A.S., 2015. Geochemical and isotopic constraints on island arc, synorogenic, post-orogenic and anorogenic granitoids in the Arabian Shield, Saudi Arabia. Lithos 220–223 (0), 97–115.

Robinson, F.A., Foden, J.D., Collins, A.S., Payne, J.L., 2014. Arabian Shield magmatic cycles and their relationship with Gondwana assembly: insights from zircon U-Pb and Hf isotopes. Earth and Planetary Science Letters 408 (0), 207–225.

Roig, J.Y., Tucker, R.D., Peters, S.G., Delor, C., Theveniaut, H., 2012. Carte Géologique de la République de Madagascar à 1/1,000,000, Ministère des Mines, Direction de la Géologie, Programme de Gouvernance des Resources Minérales.

Scherer, E., Münker, C., Mezger, K., 2001. Calibration of the lutetium-hafnium Clock. Science 293 (5530), 683–687.

Schmitt, R.S., Trouw, R.A.J., Passchier, C.W., Medeiros, S.R., Armstrong, R., 2012. 530Ma syntectonic syenites and granites in NW Namibia — their relation with collision along the junction of the Damara and Kaoko belts. Gondwana Research 21 (2), 362–377.

Schofield, D.I., Thomas, R.J., Goodenough, K.M., De Waele, B., Pitfield, P.E.J., Key, R.M., Bauer, W., Walsh, G.J., Lidke, D.J., Ralison, A.V., Rabarimanana, M., Rafahatelo, J.M., Randriamananjara, T., 2010. Geological evolution of the Antongil Craton, NE Madagascar. Precambrian Research 182 (3), 187–203.

Shackleton, R.M., 1996. The final collision between East and West Gondwana; where is it? Journal of African Earth Sciences 23, 271–287.

Sláma, J., Košler, J., Condon, D.J., Crowley, J.L., Gerdes, A., Hanchar, J.M., Horstwood, M.S.A., Morris, G.A., Nasdala, L., Norberg, N., Schaltegger, U., Schoene, B., Tubrett, M.N., Whitehouse, M.J., 2008. Plešovice zircon — a new natural reference material for U-Pb and Hf isotopic microanalysis. Chemical Geology 249 (1–2), 1–35.

Squire, R.J., Campbell, I.H., Allen, C.M., Wilson, C.J., 2006. Did the Transgondwanan Supermountain trigger the explosive radiation of animals on Earth? Earth and Planetary Science Letters 250 (1–2), 116–133.

Stern, R.A., 2002. Crustal evolution in the East African Orogen: a neodymian isotopic perspective. Journal of African Earth Sciences 34, 109–117.
Stern, R.J., 1994. Arc assembly and continental collision in the Neoproterozoic East African orogeny - implications for the consolidation of Gondwana. Annual Review of Earth and Planetary Sciences 22, 319–351.
Sun, S.S., McDonough, W.F., 1989. Chemical and isotopic systematics of ocean basalts: implications for mantle composition and processes. In: Saunders, A.D.N., M.J. (Eds.), Magmatism in the Ocean Basins. Geological Society of London Special Publication. Geological Society of London, pp. 313–345.
Thomas, R.J., De Waele, B., Schofield, D.I., Goodenough, K.M., Horstwood, M., Tucker, R., Bauer, W., Annells, R., Howard, K., Walsh, G., Rabarimanana, M., Rafahatelo, J.M., Ralison, A.V., Randriamananjara, T., 2009. Geological evolution of the Neoproterozoic Bemarivo belt, northern Madagascar. Precambrian Research 172 (3–4), 279–300.
Thompson, A.B., Connolly, J.A.D., 1995. Melting of the continental crust: some thermal and petrological constraints on anatexis in continental collision zones and other tectonic settings. Journal of Geophysical Research: Solid Earth 100 (B8), 15565–15579.
Tucker, R.D., Ashwal, L.D., Handke, M.J., Hamilton, M.A., Le Grange, M., Rambeloson, R.A., 1999. U-Pb geochronology and isotope geochemistry of the Archean and Proterozoic rocks of north-central Madagascar. The Journal of Geology 107, 135–153.
Tucker, R.D., Kusky, T.M., Buchwaldt, R., Handke, M.J., 2007. Neoproterozoic nappes and superposed folding of the Itremo Group, west-central Madagascar. Gondwana Research 12 (4), 356–379.
Tucker, R.D., Peters, S.G., Roig, J.Y., Théveniaut, H., Delor, C., 2012. Notice explicative des cartes géologique et métallogéniques de la République de Madagascar à 1/1,000,000 Ministère des Mines. PGRM, Antananarivo, République de Madagascar (in French).
Tucker, R.D., Roig, J.Y., Delor, C., Amelin, Y., Goncalves, P., Rabarimanana, M.H., Ralison, A.V., Belcher, R.W., 2011. Neoproterozoic extension in the greater Dharwar Craton: a reevaluation of the "Betsimisaraka suture" in Madagascar. Canadian Journal of Earth Sciences 48 (2), 389–417.
Tucker, R.D., Roig, J.Y., Moine, B., Delor, C., Peters, S.G., 2014. A geological synthesis of the Precambrian shield in Madagascar. Journal of African Earth Sciences 94 (0), 9–30.
Turner, S.P., Foden, J.D., Morrison, R.S., 1992. Derivation of some A-type magmas by fractionation of basaltic magma: an example from the Padthaway Ridge, South Australia. Lithos 28 (2), 151–179.
Valley, J.W., 2003. Oxygen Isotopes in Zircon. Reviews in Mineralogy and Geochemistry 53 (1), 343–385.
Valley, J.W., Kinny, P.D., Schulze, D.J., Spicuzza, M.J., 1998. Zircon megacrysts from kimberlite: oxygen isotope variability among mantle melts. Contributions to Mineralogy and Petrology 133 (1–2), 1–11.
Valley, J.W., Lackey, J.S., Cavosie, A.J., Clechenko, C.C., Spicuzza, M.J., Basei, M.A.S., Bindeman, I.N., Ferreira, V.P., Sial, A.N., King, E.M., Peck, W.H., Sinha, A.K., Wei, C.S., 2005. 4.4 billion years of crustal maturation: oxygen isotope ratios of magmatic zircon. Contributions to Mineralogy and Petrology 150 (6), 561–580.
van Staal, C.R., Whalen, J.B., Valverde-Vaquero, P., Zagorevski, A., Rogers, N., 2009. Pre-Carboniferous, episodic accretion-related, orogenesis along the Laurentian margin of the northern Appalachians. Geological Society, London, Special Publications 327 (1), 271–316.
Veevers, J.J., 2017. West Gondwanaland during and after the Pan-African and Brasiliano orogenies: downslope vectors and detrital-zircon U-Pb and TDM ages and εHf/Nd pinpoint the provenances of the Ediacaran–Paleozoic molasse. Earth Science Reviews 171, 105–140.
Vermeesch, P., 2012. On the visualisation of detrital age distributions. Chemical Geology 312–313 (0), 190–194.
Viola, G., Henderson, I.H.C., Bingen, B., Thomas, R.J., Smethurst, M.A., de Azavedo, S., 2008. Growth and collapse of a deeply eroded orogen: insights from structural, geophysical, and geochronological constraints on the Pan-African evolution of NE Mozambique. Tectonics 27 (5), 2008TC002284.
Whalen, J., Currie, K., Chappell, B., 1987. A-type granites: geochemical characteristics, discrimination and petrogenesis. Contributions to Mineralogy and Petrology 95 (4), 407–419.
Zhou, J.-L., Rasoamalala, V., Razoeliarimalala, M., Ralison, B., Luo, Z.-H., 2015. Age and geochemistry of Early Cambrian post-collisional granites from the Ambatondrazaka area in east-central Madagascar. Journal of African Earth Sciences 106 (0), 75–86.